Arab American University

Faculty of Graduate Studies

Relaxation Dynamics of QDLs Subjected to External Effect (Optical Feedback)

By

Haneen Noman Mohamad Jaradat

Supervisor

Assoc. Prof. Dr. Muayad Abu Saa

Co-Supervisor

Assoc. Prof. Dr. Adli Saleh

This thesis was submitted in partial fulfillment of the requirements for the Master's degree in Physics

March/2024

Thesis Approval

Relaxation Dynamics of QDLs Subjected to External effect

(Optical Feedback)

By

Haneen Noman Jaradat

This thesis was defended successfully on March 4th 2024 and approved by:

Committee members	Signature
1. Assoc. Prof. Dr. Muayad Abu Saa: Supervisor	……
2. Assoc. Prof. Dr. Adli Saleh: Co- Supervisor	……
3. Assist. Prof. Dr. Suleiman Rabba: Internal Exam	……
4. Prof. Dr. Mohammad El-Said: External Examiner	……

Declaration

The work provided in this thesis, unless otherwise referenced, is the researcher's own work, and has not been submitted elsewhere for any other degree or qualification.

Student's Name: Haneen Noman Jaradat

Student ID: 202113364

Signature: 

Date: May 16th 2024.

Dedication

To My Parents

Acknowledgments

First and foremost, I thank Allah, the Almighty, for providing me with this opportunity and equipping me with the necessary skills to make it a success. The current form of my thesis is the result of the advice and assistance of many people. As a result, I'd like to express my gratitude to everyone.

I am eternally grateful to my supervisors, Dr. Muayad Abu Saa and Dr. Adli Saleh, whose views and feedback were vital throughout this trip.

I would like to thanks my colleagues, who supported me and put up with my stresses and moans for the past two years of study

I also extend my appreciation to my parent for their unwavering encouragement, to my daughters Saja and Yaqeen and my brothers Baha', Día' and Mohammad for their continuous support.

To my precious twins, Sara and Maryam and my husband Mohammad, thanks for all your support and patience without which I would have stopped these studies long time ago.

I would like to express my deepest appreciation to all those who provided me the possibility to complete this work.

Abstract

In this study, we examine quantum dot lasers (QDLs) that utilize quantum dots as the active medium. QDLs work on the principle of tight confinement of charge carriers in quantum dots, and find a wide range of applications in medical imaging, sensing, quantum information processing and optical communications. Due to their vital role in optical communication and optical tomography in addition to the ability of high rates of data processing, new approaches are employed to enhance their performance. Our work focuses on the theoretical treatment of the optical feedback effects on the dynamics of QDLs using a rate equation approach. Analytical expressions for both relaxation oscillation (RO) frequency and damping rate are derived. In addition, the simulation method is used to compare our results with that for solitary lasers. It is found that optical feedback strengthens RO frequency and reduces the damping rate and factor as the injection rate increases, which indicates the decrease in system stabilities. Furthermore, a region of instabilities implies by positive damping rate is observed. Moreover, for negative detuning frequency, there is a region of bistability which makes the laser capable to use as optical switch and in optical data storing.

Table of contents

List of Tables

List of figures

List of Symbols

Symbol	Symbol Meaning
N_2	Carrier density in higher atomic quantum state
E_2	Energy in higher atomic quantum state
E_1	Energy in lower atomic quantum state
k_B	Boltzman constant
N_1	Carrier density in lower atomic quantum state
T	Temperature
n_r	Effective refractive index
α_i	Internal loss per unit length
L	Cavity length
R_1	First mirrors reflectivity
R_2	Second mirror reflectivity
τ	Carrier life time
τ_{nr}	Non-radiative recombination life time
τ_r	Radiative recombination lifetime
τ_p	Photon life time
ω_{RO}	Relaxation oscillation frequency
a	Differential gain
v_g	Group velocity

V_P	Volume occupied by photon
η_i	Quantum efficiency
i	Injected current
i_{th}	Threshold current
Γ_{RO}	Damping rate
$\Upsilon G(N)$	The power gains
Υ	Confinement factor
G	Gain coefficient
N	The population inversion
T_C^{-1}	Decay rate due to the loss of photons by mirror transmission and scattering
T_1^{-1}	Decay rate of the population
N_0	The population difference in the absence of laser light
R_p	The pumping rate
τ_p	The photon life time
$\omega(N)$	Cavity resonance frequency
ω_0	Optical frequency
J	Pump current
τ_S	Carrier lifetime.
I	Intensity of the laser field in the cavity
ρ	Occupation probability
n	Number of the carrier in the wetting layer
$\Phi(t)$	Phase of electric field

η	Ratio of the carrier and photon decay rate
$F(\rho, n)$	Function describe the carrier exchange rate between the wetting layer and the dot
I_S	Steady state intensity
α	Linewidth enhancement factor
Γ	Injection rate
Δ	Detuning frequency which defined as the frequency of the master laser minus the frequency of slave laser
B	Capture rate
τ	The carrier recombination time
τ_{cap}	The capture times
η	Ration between photon lifetime τ_{ph} and the recombination time τ
$1-\rho$	The Pauli blocking factor
K	Damping factor
γ_0	Inverse of the differential carrier lifetime
ω_L	Frequency of the laser reflected back into the cavity
ω_0	Resonance frequency of the cavity

Acronyms

Acronyms	Acronyms meaning
FRI	Far infrared
SCL	Semiconductor laser
RIN	Relative intensity noise
QW	Quantum well
QWires	Quantum wires
QD	Quantum dot
QDLs	Quantum dot lasers
EEL	Edge emitting laser
RO	Relaxation oscillation
VCSEL	Vertical cavity surface emitting layer
DH	Double heterostructure
DWell	Dot in well
MBE	Molecular beam epitaxy
MOCVD	Metal-organic chemical vapor depositon

Chapter One

Introduction

1.1 The LASER:

The word laser is an acronym for Light Amplification by Stimulated Emission of Radiation. The output power of laser light varies from a few thousandths of a watt such as in laser pointers to several thousand watts as in industrial laser cutters. Laser light has several properties that make it possible to be used in several fields of technology such as in medical applications like laser surgery [1], laser industry as laser drilling [2] and other applications such as barcode readers and laser pointers [3]. Laser light is characterized by being monochromatic, which means it emits light with a narrow range of wavelengths due to stimulated emission. Additionally, laser light is directional, traveling in a specific path with minimal dispersion. Furthermore, it is coherent, signifying a sustained phase relationship among its waves as they travel through both space and time. Coherence manifests in two forms: temporal coherence, emphasizing consistency over time, and spatial coherence, highlighting a stable phase relationship in terms of space [4]. These properties of laser light enable it to deposit a lot of energy in small areas, making it more hazardous than ordinary light [5].

Light amplification and laser operation mainly depend on stimulated emission. In order to understand how lasing occurs, we need to understand the mechanisms of light interaction with atoms or molecules. The energy levels of atoms and molecules are quantized. The particle of a higher quantum energy state (E_2), and a lower energy state (E_1) can interact

with light of energy $h\upsilon = E_2 - E_1$. Einstein identified three processes in which particles exchange energy [6], as shown in figure 1 [7]. These processes are:

1. Absorption:

   An incident photon is absorbed by the particle, causing an electron to jump from a lower energy level $E_1$to a higher one E_2.

2. Spontaneous emission:

   A particle in an upper level E_2 can decay spontaneously to a lower level E_1 and emits a photon.

3. Stimulated emission:

   This process involves the interaction of an incoming photon with an excited electron in the particle, which prompts the electron to transition to a lower energy state, resulting in the emission of a photon. It is important to note that the characteristics of the emitted photon are indistinguishable from those of the incident photon.

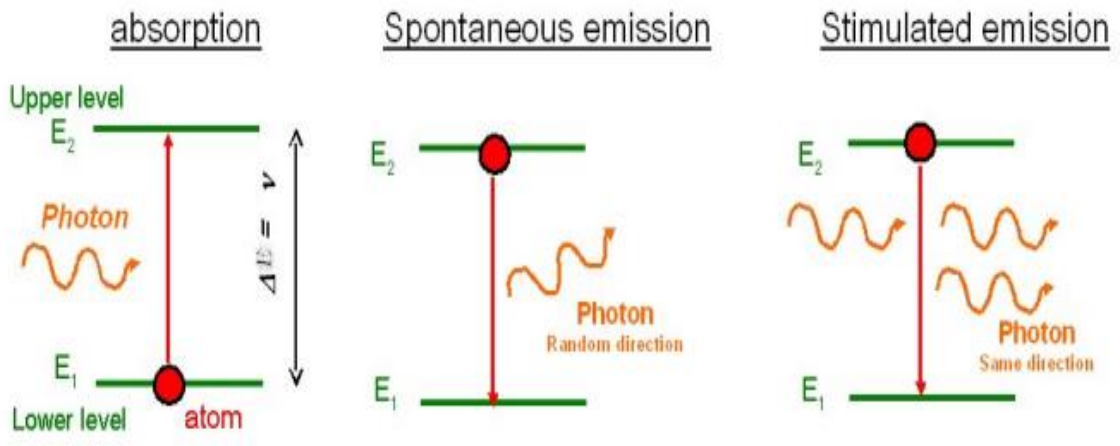

Figure 1.1: Schematic illustration of radiation process: absorption, stimulated emission and spontaneous emission [7].

All conventional lasers have three essential elements, as shown in figure 1.2 [8]:

• Gain or active (amplifying) medium:

It depends on the type of laser, it may be gas, liquid or solid. When the gain is appropriately energized, it allows the creation of population inversion, which involves maintaining a higher number of particles, in the excited state than in the ground state. This condition is essential for the amplification of the light.

• The pump source:

Also known as the energy source, plays a vital role in supplying energy to the gain medium, leading to the excitation of its atoms or molecules. Its essential function is to initiate and sustain the process required to achieve population inversion.

• Cavity (optical resonator):

In most cases, cavity consists of two parallel mirrors, causing photons reflect back and forth several hundred times before exiting the resonator. One of the mirrors is partially transparent, facilitating the emission of the laser beam output.

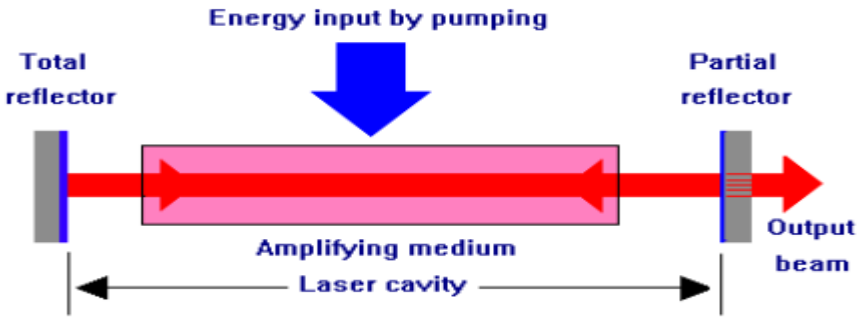

Figure 1.2: Scheme of the essential elements of conventional laser [8].

Lasing occurs when the number of photons produced by the stimulated emission of light exceeds the number of photons absorbed. Lasing requires a higher population inversion at the upper energy level (N_2) than the population inversion at the lower energy level (N_1). However, at thermal equilibrium, the number of atoms at the lower energy level (E_1)is larger than that at the upper energy level (E_2), according to [9]:

$$N_2 = N_1\, e^{-(E_2-E_1)/k_BT} \qquad 1.1$$

Where k_B is the Boltzmann constant and T is the temperature in Kelvin.

Population inversion can be achieved by adding energy using different pumping systems. It may be electrical, optical [10], x-ray pumping [11], e-beam pumping [12] and chemical pumping [13]. The two most commonly used pumping system are optical and electrical pumping. In both systems, the pumping energy must match the difference in energy between the excited state and the ground state. In optical pumping, a two-level system is theoretically possible under certain conditions, but achieving population inversion is not very practical. In this system, the occurrence of stimulated emission results in the emission of a photon, causing the particle to return to the ground state. This process depletes the population of particles in the excited state, making it challenging to achieve and sustain population inversion. In three and more level system, there is an additional intermediate state between the excited and ground state as shown in figure 1.3 [14]. These intermediate states provide enhanced flexibility in both excitation and relaxation processes. The absorption of photons during optical pumping can temporarily fill these intermediate states, establishing a reservoir of particles that actively participate in the population inversion process. Optical pumping is

suitable for solid state lasers like Ruby [5], while electrical pumping is suitable for gas lasers [15].

Figure 1.3: Three-level laser energy diagram [14].

1.2 Laser Types

Categorizing lasers based on their amplifying medium yields three main types:

1. Gas lasers which use a low-pressure gas mixture as an active medium with the electrical pump source commonly used. Helium Neon (He-Ne) laser stands out as one of the most frequently utilized examples in this category.

2. Liquid lasers employ a liquid as their active medium, with an optical pump source being utilized. A representative example of a liquid laser is the dye laser, which incorporates organic material as its active medium.

3. Solid- state laser: in these laser glass or crystalline material acts as the host and doped with rare earth element impurity (Nd^{+3}, Yb^{+3}, Er^{+3}, Ti^{+3}) [16], Optical pumping serves as the

pump source for these lasers. Among them, the Neodymium-doped Yttrium Aluminum Garnet (Nd:YAG) laser stands out as the most frequently utilized [17]. Additionally, solid-state lasers encompass semiconductor lasers, where the p-n junction acts as the active medium. Common examples of semiconductor lasers are GaN, GaAlInP and AlGaAs.

1.3 Laser Dynamics

There are three dynamical variables used to describe the dynamics of most lasers: the electric field, the material polarization and the population inversion. The more rapid decaying variables are adiabatically eliminated. According to the number of required variables to describe laser operation, the following classification have been introduced [18]:

- Class A: one single nonlinear electric field describes the laser; both polarization and population inversion are adiabatically eliminated because they have a much shorter decay time. example: gas laser [He-Ne laser] [19] and dye laser.
- Class B: the dynamics of lasers ruled by electric field and population inversion. Material polarization is adiabatically eliminated since it follows the field without decay. example: Ruby Laser [20].
- Class C: involve the simultaneous use of all three variables to describe their operation. No adiabatic elimination is employed in Class C lasers because the decay times of these three variables are comparable. An illustration of a Class C laser is the Far Infrared (FIR) laser [21].

1.4 Semiconductor Lasers

1.4.1 Semiconductor Band Structure:

The lower energy level in semiconductors is called the valence band VB and the higher energy level is called the conduction band CB. The difference between the top of VB and the bottom of CB is called the band gap E_g . Semiconductors band gap ranges between 0 and $3\ eV$ [22]. When the temperature is higher than $0K^{\circ}$, thermal excitation causes electrons to rise from VB to CB leaving holes in the VB. Both electrons and holes contribute to electrical conductivity.

There are two types of band gaps in semiconductors:

1. Direct band gap:

   The top of the VB and the bottom of the CB have the same crystal momentum, and an electron directly can emit the photon since it occurs at the same momentum.

2. Indirect band gap:

   The top of the VB and the bottom of the CB don't occur at the same momentum, which means that the electron must interact with both phonons and photons to verify the conservation of both energy and momentum. A direct band gap is preferable in a laser field since the rate of stimulated emission is larger than that in an indirect band gap.

1.4.2 Semiconductor Lasers (Diode Laser) SCLs

Semiconductor lasers have an important technological role since their invention in the early 1960s [23]. They are used in different applications such as medical, welding [24], computer interconnects and bar-code readers [25]. Also, they are widely used in optical communication because they are compact, low cost and efficient [26]. In addition, they are used in telecommunication application, CD-ROMS, DVD and printer [27]. The reasons behind the wide range usage of SCLs are their small size, low cost, large modulation band width [28], low electrical power consumption [29] and their continued performance improvements especially in low-threshold current.

SCLs usually consist of a p-n junction, where electrons diffuse from the n-side to the p-side and holes diffuse from the p-side to the n-side. This diffusion results in the formation of a potential difference between the two regions, subsequently preventing further movement of electrons from the n-side to the p-side. By applying a forward bias voltage which is positive on the p-side and negative on the n-side across this pn-junction, carriers are diffuse across the junction. Consequently, electrons and holes recombine, releasing photons.If another photon with the same energy interacts with the excited electron, it can stimulate the release of second photon with identical property.

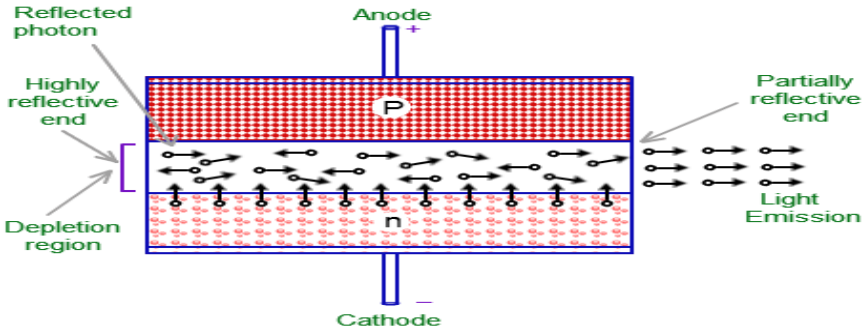

Figure 1.4: Scheme of p-n junction SCLs [30].

The optical resonator is formed by cleaving the substrate along the crystal as shown in figure 1.4 [30]. These bulk SCLs could only operate at low temperatures, and their lifetimes were too short for application.

To achieve efficient recombination of electron and hole, heterostructures are formed at both interfaces by sandwiching undoped semiconductor material with a small energy band gap and high refractive index between n-doped and p-doped semiconductor material forming a p-i-n junction. Under a forward bias, the holes are injected from the p region to the sandwiched region, and the electrons are injected from the n-region to the sandwiched region. The refractive index of the sandwiched region is usually greater than that of the p and n regions. As a result, potential well will be formed and a large number of carriers will be efficiently confined to the active sandwiched region, resulting in a high light amplification rate. It is important to notice that the first continuous wave (CW) laser oscillation at room temperature was achieved by the double heterostructure [31, 32]. SCLs are mass produced using depositing various layers by lithographic techniques. They are small, very efficient lasers with dimensions of less than a millimeter. Semiconductor lasers range in wavelength from 0.4–1.8 μm [33, 34] with typical continuous output powers up to 100 mW. Usually, the thickness of the sandwiched layer is of order 100 nm. New fabrication technique allows the reduction of the sandwiched layer thickness to the scale of, or even less than, the DeBroglie wavelength. Consequently, the energy state splitting into sub-bands, resulting in a quantum well (QW) laser heterostructure. In this configuration, carriers are confined to a square potential well in the transverse dimension while remaining free in the other dimension. In the QW laser, injected carriers accumulate near the bottom of CB and the top of VB,

concentrating into sub bands. This leads to a significant number of carriers contributing to lasing action. QWLs operate at room temperature [35], require a lower threshold current and offer narrower spectral linewidth, greater temperature stability and increase optical gain. The most common QWLs are fabricated from GaAs/AlGaAs and InGaAsP/InP structures. QWLs find their applications in optoelectronics, medical therapy, material processing and laser printing [36, 37]. Confinement of the carrier in two spatial directions is also possible, which results in quantum wire (QWire). Despite their potential advantages, such as unique electronic and optical properties, QWires have not gained widespread use in semiconductor photonics. This is mainly attributed to the lack of efficient growth techniques that would enable their fabrication with sufficiently high densities. When carriers are confined in all three spatial directions on a scale smaller than the de Broglie wavelength, quantum dot lasers (QDLs) emerge, featuring truly discrete energy levels [38]. It offers further threshold reduction and higher temperature stability [39, 40]. Figure1.5 [41] shows the density of state for bulk semiconductors, quantum wells, quantum wires and quantum dots.

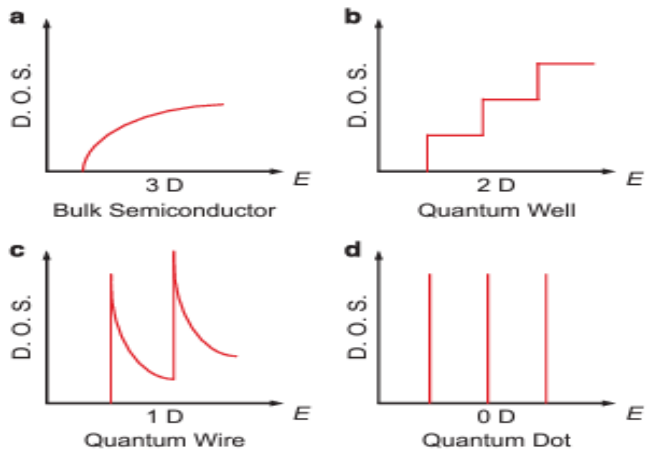

Figure 1.5: density of state for bulk, quantum well, quantum wire and quantum dot structure [41].

There are two configurations for laser emission in semiconductors:

1. Edge emitting laser (EEL): light propagates in a direction parallel to the surface of a semiconductor. To create this laser, the wafer is cleaved at both ends and coated with a mirror. It can host multiple modes of simultaneous action.

2. Vertical cavity surface emitting laser (VCSEL): light propagates in a direction perpendicular to the surface of the semiconductor. The resonator uses two semiconductor Bragg mirrors. It offers a lot of advantages in terms of testing, stability, and cost effectiveness.

1.4.3 SCLs Dynamics

SCLs are characterized by a time scale separation between the fast photon and the slower carrier. Operating as a class B laser, SCLs are governed by two dynamic variables: the complex electric field and the population inversion. Adiabatic elimination is applied to eliminate material polarization due to its rapid decay [42]. The complex electric field consists of both a real part, representing amplitude, and an imaginary part, signifying phase. Thus, understanding laser operation requires examining the amplitude and phase of the field, along with the population inversion. For a free running single mode laser, the dynamics of intensity and population inversion are decoupled since the phase varies very quickly [43]. The dynamics of SCLs are very sensitive to the external effects such as optical feedback effect, it

resulting in instabilities in laser output. These dynamical instabilities hold significance in applications like secure communication and radar systems [44].

1.5 Carrier and photon lifetimes

Carrier life time is defined as the average time required for minority carrier to recombine. It associated with radiative recombination lifetime (τ_r) and non-radiative recombination lifetime (τ_{nr}) by [45]:

$$\frac{1}{\tau} = \frac{1}{\tau_r} + \frac{1}{\tau_{nr}} \tag{1.2}$$

Photon lifetime (τ_p) expresses the rate at which photons are lost from the cavity, it is given by [45]:

$$\frac{1}{\tau_p} = \frac{c}{n_r}\left[\alpha_i + \frac{1}{2L}\ln\left(\frac{1}{R_1 R_2}\right)\right] \tag{1.3}$$

Where: n_r: effective refractive index, α_i: internal loss per unit length, L: cavity length, R_1 , R_2: mirrors reflectivities.

The first term stands for losses due to propagation in the cavity material, while the second term is concerned with mirror losses. Both times, τ_p and τ in SCLs have an important role in the dynamical behavior of the laser and they are related to the relaxation oscillation RO. The carrier lifetimes affect the rate at which the population inversion occur. A short carrier lifetime results in faster recombination, subsequently impacting laser response. A long photon lifetime leads to a more accumulation of photons in the cavity, results in a more sustain and stable laser.

1.6 Gain and Threshold Current

The gain refers to the amplification of light in laser results from stimulated emission. To attain gain, population inversion must be achieved and sustain. However, the laser cavity is not perfect environment and losses occur as mentioned previously. These losses may be due to propagation in the cavity such as absorption of photons by the cavity material, imperfection in the material or scattering of photon, Also the losses may be due to imperfect mirrors, which can lead to absorption or scattering losses. For lasing to occur sufficiently, the gain must exceed the losses. The minimum current required to initiate the laser is called threshold current, before threshold current the laser output is not sustain. Once the threshold current is exceeded, a continuous and coherent laser output is achieved.

1.7 Relaxation Oscillation

Relaxation oscillation (RO) in output power and the corresponding damping rate are important characteristics of different types of lasers. RO occurs when the laser is in operation within a low threshold current region. Upon activation, lasing is not achieved immediately since it requires some time for carrier concentration to build up and accumulate, consequently, photons also need some time to reach a steady state, resulting in an output oscillation called RO. RO occurs in all B class lasers since the upper state life time is often larger than the laser resonator damping time. Conversely, lasers in the class A region, where an upper state life time is shorter than the laser cavity damping time, do not exhibit RO. Instead, they exhibit only exponential relaxation to the steady state [42].

Understanding of the RO of a laser has an important role in determining the number of fundamental variables and enabling predictions of laser behavior under certain operation modes. Single mode SCLs which emits light in only one spatial or temporal mode exhibits strong relaxation oscillations in the gigahertz region and they are slowly damped. When SCLs are subjected to external forcing such as optical injection and optical feedback, they are sustained.

The RO frequency (ω_{RO}) increases by increasing the injected current above the threshold region according to the formula [46]:

$$\omega_{RO}^2 = \frac{a v_g \eta_i}{q V_P}(i - i_{th}) \qquad 1.4$$

Where a: $\frac{\partial g}{\partial \mathrm{N}}$ the differential gain, g: the gain factor per unit length, N: Carrier density, v_g: group velocity of light in laser cavity, q: electron charge, V_P volume occupied by photons in the cavity, i, i_{th}: injected and threshold current.

The RO damping rate (Γ_{RO}) is a measure of how quickly oscillations in a system decay or decrease after being perturbed. A higher damping rate means that the system returns to its equilibrium or steady state more rapidly. On the other hand, a lower damping rate resulting in a more sustained oscillations or a longer time for the system to reach a stable state. Damping rate (Γ_{RO}) is Directly proportional to RO frequency (ω_{RO}^2) according to the following formula [45]:

$$\Gamma_{\mathrm{RO}} \propto K\, \omega_{RO}^2 \qquad 1.5$$

Where K related to maximum modulation band width. The maximum modulation band width refers to the range of frequency over which the laser can effectively response to the input signal. The modulation of the band width represents the ability of the laser to track and transmit rapidly changing signals. Modulation band width has important roles in optical communication systems directly influencing the speed and capacity of data transmission.

1.8 Optical Feedback

Optical feedback is achieved by returning part of the coherent laser radiation that was created inside the active medium, back. Usually, it is done by using mirrors at both ends of the active medium. The effects of optical feedback in semiconductor lasers have been studied since the beginning of their development by Risch and Voumard in 1977 [47]. In 1982 Lang and Kobayashi published a paper on effects of the optical feedback in the dynamical properties of SCLs using a distant mirror [48]. Since then, researchers have directed their efforts to study and understand the induced dynamics due to optical feedback. Self-optical feedback has been used in SCLs in order to control RO frequency, frequency stability, and mode selection. It is found that at a certain condition, optical feedback causes a reduction in linewidth of output power, turnability and improvement of coherence. On the other hand, instabilities in the laser output have been appeared under the optical feedback of SCLs.

The dynamics of SCLs under optical feedback are very important in practical applications especially in optical systems such as optical communication, optical data storage and optical measurements.

The static behavior of SCLs under optical feedback can be theoretically investigated depending on the level of feedback, gain media, injection current and other laser parameters. Tkach and Chraplyvy investigated the instabilities of SCLs with optical feedback and categorized them into five regimes depending on the feedback fraction [49]. The dynamic characteristics of SCLs under optical feedback are described by the time-dependent rate equation. A lot number of papers have been published about the dynamical response of SCLs to optical feedback, ranging from chirp reduction, over a reduction of relative intensity noise (RIN) to larger bandwidth under direct optical modulation. It was also studied under delayed optical feedback to study the stabilization of steady state and periodic orbits [50, 51].

1.9 Quantum Dot Lasers QDLs

One major advantage of quantum dot structures results from their unique and delta-like discrete density of energy state due to three-dimensional spatial carrier confinement at the nanoscale. Ideal QDLs are expected to have many interesting and useful properties such as very low threshold current density, high temperature stability, high differential gain, wide modulation bandwidth and low power consumption. QDLs have a significant role in telecommunications, biomedical applications [52], photonic technologies [53] and optoelectronic applications such as solar cells, optical amplifiers [54], optical data storages [55] and random number generators [56].

In 1963 Kromer et al. [57] and Alferov et al. [58] proposed the idea of carrier confinement using double heterostructures (DH). In the 1970s Dingle and Henry recognized that wavelength tuneability and threshold reduction can be realized in quantum structured SCLs

[59]. Theoretically this was proven by Asada et al and Arakawa et al in the 1980s [60]. It was not until the early 1990s that self-assembled QDs could be fabricated by epitaxial growth techniques [61-63]. The first QDLs self-assembled QDs were successfully fabricated and operated at low temperatures up to $77K^{\circ}$ in 1994 [64]. Subsequent years, researchers and engineers explored new fabrication methods and various semiconductor material to improve the performance and efficiency of QDLs material.

QDs can be fabricated using different methods. Three mainly used methods are:

1. Epitaxial growth:

QDs are epitaxial grown by the Stranski–Krastanov growth method using standard molecular beam epitaxy (MBE) or metal-organic chemical vapor deposition (MOCVD) techniques [66]. It allows for the spontaneous synthesis of three-dimensional nanostructures during strained layer hetero-epitaxial growth, which results from mismatch between the substrate and the epilayer. In this process, a thin film of certain material such as III–V and II–VI materials are grown layer by layer on a semiconductor substrate such as GaAs and InP, which is called the wetting layer (WL) until a certain critical thickness is reached. After that, the planar growth of the film stops and three-dimensional islands of variable size across the plane begin to form spontaneously due to strain relaxation and thus self-assembled which become a self organized QD. It can have very small dimension ($< 10\ nm$). Also, there is another structure known as the dots-in-the-well Dwell, where each layer of QDs resides inside a thicker QW, with the thickness of a well exceeding the height of the dots [67]

2. Micro crystallites in glass or polymer:

By poring nanoparticle into molten glass or polymer and cooling them down

3. Artificially patterned dots by electron-beam lithography.

In QD devices, the carriers are injected into a surrounding carrier reservoir witting layer (WL or QW) before they scatter into QD. The scattering rate depends on the energy spacing between the band edge of QW and the energy level of QD. This energy difference determines the life times of the carrier in QD. If the energy spacing is small, the carrier life times are shorter than the photon lifetime and acts as a class A laser. For large spacing energy, the time scale of femtosecond between photon life time and carrier life time results and act as a class B laser. Between these two limiting cases, QD exhibits dynamical feature of both classes A and B.

1.10 QDLs Subjected to Optical Feedback

QDLs have shown lower sensitivity to optical feedback compared to other SCLs [68], enabling them to operate in the absence of a highly expensive isolator. Isolators are typically needed to avoid unwanted reflection that can lead to temporal instabilities of the lasers. If chaos is induced by the feedback, it can be utilized for secure chaos communication and chaos key distribution [69]. Several studies have concentrated on the nonlinear dynamics of QDLs under external perturbations [70, 71]. Under optical injection, bistability has been observed in QDLs. At moderate level of optical feedback and pumping current near threshold current, low-frequency fluctuation LFF has been observed experimentally and theoretically

[72, 73]. Unlike bulk or QW semiconductor lasers, QDLs have symmetric gain curves and experiments have demonstrated very small phase-amplitude coupling (α-parameter) [74].

Chapter Two

Rate equations

2.1: Introduction

Modeling lasers requires a full quantum treatment, but many dynamical properties may be realized by semi classical or purely classical approaches. The basic framework to extract analytically as much information as possible is provided by rate equations, which have long been used to model the output power and the oscillation of lasers. The rate equations give the rate at which populations of different energy levels change due to the pump and in the presence of laser radiation. In addition, they provide the time dependence of the atomic populations of various levels in the presence of radiation at frequencies corresponding to the different transitions of the atom and the steady-state population inversion between the actual levels involved in the laser transition and whether an inversion of population is achieved in a transition or not. And if so, what would be the minimum pumping rate required to maintain a steady population inversion between the two levels.

The most basic processes involved in laser operation are two-level system ground and excited level E_1 and E_2 with number of atoms N_1 and N_2 respectively. The process of light-matter interaction is restricted to stimulated emission and absorption. The rate equation for photon number n and populations N_1 and N_2 are [75]:

$$\frac{dn}{dT} = GNn - \frac{N}{T_C} \tag{2.1}$$

$$\frac{dN}{dT} = -\frac{1}{T_1}(N - N_0) - 2GNn \tag{2.2}$$

Where T: time included radiative and nonradiative, G: the gain coefficient for stimulated emission, $N = N_2 - N_1$: the population inversion, T_C^{-1} : the decay rate due to the loss of photons by mirror transmission and scattering, T_1^{-1} : the decay rate of the population and $N_0 = R_p T_1$ is the population difference in the absence of laser light and R_p is the pumping rate.

For single mode SCLs the appropriate rate equation requires more description of active medium. Taking into account the complex amplitude of optical electric field $E_{OPP}(\tau) = E(\tau)\exp^{i\omega\tau}$ [75], the rate equation becomes:

$$\frac{dE}{d\tau} = \frac{1}{2}(\Upsilon G(N) - \tau_P^{-1})E + i(\omega(N) - \omega_0)E \quad 2.3$$

$$\frac{dN}{d\tau} = \frac{J}{e} - \frac{N}{\tau_S} - G(N)E^2 \quad 2.4$$

Where τ denotes the real physical time, $\Upsilon G(N)$ defined as the power gain, the parameter Υ called the confinement factor, τ_p: the photon life time, $\omega(N) - \omega_0$ is the detuning between the cavity resonance frequency and the optical frequency, J is the pump current, τ_S is the carrier lifetime.

A better description of the electric field $E(\tau) = Re(E_0(\tau)\exp^{i(\omega\tau+\Phi)})$ where the phase Φ must be considered in some experiment. Especially, when there exists an optical time frequency reference such as when the laser is injected with the field of another laser the phase between two sources must be considered.

In practice, lasers are realized in three- and four-energy level system, where the light matter interaction is described by population equations for all levels contributed to the laser

operation and the rate equation is more complicated. Using a two-level system, three or four level system depend on the nature of the active medium. The solution of three or four level rate equations differs slightly from the solution of standard rate equation SRE (two-level system) as mentioned in equations (2.3) and (2.4) and the dynamical response of many laser depends on dynamical features that can be captured by SRE.

2.2 Rate equation models used for QDLs

The dynamical behavior of QDLs was investigated using a wide range of approaches and models. The simple models are based on rate equations. In QDLs, carriers are injected into the wetting layer before being captured by the dot, so we need to introduce the occupation probability of the dot in addition to the electric field in the cavity and the carrier density in the wetting layer and we need to consider the carrier capture process and pauli blocking. A.V.Uskov et al analyzed QDLs with those three variable rate equations and considered that the carriers are delivered to lasing levels through Auger capture only [76]. A lot of efforts have been directed toward formulating a more suitable rate equations for QDLs. An alternative to the three-variable model, the modified two-variable QW rate equation was used for QD in [77], but it is limited to large capture rates and not sufficient if the dot is saturated by carriers [78]. In addition, a five-variable rate equation that considers the microscopic kinetic equation, which is dominant by coulomb scattering process and spontaneous emission was simulated numerically in [79], but it is too complex for an analytical understanding of QDLs dynamics.

In this work, we will apply appropriate rate equations to analyze the dynamics of QDLs under optical feedback, develop an expression for the relaxation oscillation RO and damping rate, and compare it to those found by Thomas Eraneux's for solitary QDLs [78]. The following two parts discuss both Eraneux's work and the model we will adopt.

2.3 Solitary QDLs model and dynamics

Thomas Eraneux et al analyzed a solitary QDLs using a three-variable rate equation model. They used the rate equations formulated by O'Brien et al [80], which consist of three equations for the intensity(I) of the laser field in the cavity, the occupation probability (ρ) and the number of the carrier (n) in the wetting layer. The equations are:

$$I' = [-1 + g(2\rho - 1)]I \tag{2.5}$$

$$\rho' = \eta[F(\rho, n) - \rho - (2\rho - 1)I] \tag{2.6}$$

$$n' = \eta[J - n - 2(F(\rho, n)] \tag{2.7}$$

Where g: gain factor, η: the ratio of the carrier and photon decay rate, $F(\rho, n)$: function describe the carrier exchange rate between the wetting layer and the dot.

They derived analytically expressions for both the relaxation oscillation RO frequency (ω_{RO}) and the damping rate (Γ_{RO}) as follow:

$$\omega_{RO} = (2\eta\, I_S)^{\frac{1}{2}} \tag{2.8}$$

$$\Gamma_{\mathrm{RO}} = \frac{\frac{\eta}{2}(1 + I_S)}{1 - g^{-1}} \tag{2.9}$$

Where I_S is the steady state intensity.

2.4 Full Rate Equation Model of QDLs in presence of optical feedback

Rate equations for QD laser subjected to optical feedback are given by D. Goulding [81]

$$E' = \frac{1}{2}(1 + i\alpha)[-1 + g(2\rho - 1)]E + \mathrm{r}e^{i\Delta t} \tag{2.10}$$

$$\rho' = \eta[Bn(1 - \rho) - \rho - (2\rho - 1)E^2] \tag{2.11}$$

$$n' = \eta[J - n - 2Bn(1 - \rho)] \tag{2.12}$$

where the prime means differentiation with respect to $t = \frac{t'}{\tau_{ph}}$. t': is the dimensionless unit time, α is the linewidth enhancement factor. Γ : injection rate. Δ : detuning frequency which is defined as the frequency of the master laser minus the frequency of slave laser. The last term in equation (2.10) represents the contribution of optical feedback. $B = \tau\tau_{cap}^{-1}$ Dimensionless capture rate, where τ is the carrier recombination time and τ_{cap} is the capture time. $\eta = \tau_{ph}\tau^{-1}$ is the ratio between photon lifetime τ_{ph} and the recombination time τ. The factor $1 - \rho$ is the Pauli blocking factor. The factor 2 in equation (2.10) accounts for the spin degeneracy in the QD energy level.

In the next chapter, the rate equations governing the dynamics of QDLs under optical feedback will be analyzed. This involves examining the effect of small perturbation around the steady state condition by taking derivatives of the rate equations and setting them equal to zero to find the steady state condition. After that, the partial derivative with respect to the

state variables will be used to construct the jacobian matrix. The characteristic equation will be applied to evaluate the eigenvalues of this matrix at the steady state. These eigenvalues will provide valuable insight about relaxation oscillation and damping rate.

Chapter3:

Results and Discussion

3.1 Analytical analysis

3.1.1 Reduced Rate Equation Model

The analytical investigation represented here are based on the model given in section 2.4. We introduce: $\epsilon = g - 1, \rho = 1 + \epsilon u,\ s = \epsilon t, \gamma = \epsilon^{-1}\Gamma\ , \delta = \epsilon^{-1}\Delta$

Then we obtain the following equations

$$\frac{dE}{ds}\frac{ds}{dt} = \frac{1}{2}(1 + i\alpha)[-1 + (1 + \epsilon)(2(1 + \epsilon u) - 1)]E + \gamma\epsilon e^{i\epsilon\delta\epsilon^{-1}s} \quad 3.1a$$

$$E'\epsilon = \frac{1}{2}(1 + i\alpha)[2u\epsilon(1 + \epsilon)]E + \gamma\epsilon e^{i\delta s} \quad 3.1b$$

$$E' = \frac{1}{2}(1 + i\alpha)[2u(1 + \epsilon)]E + \gamma e^{i\epsilon\delta\epsilon^{-1}s} \quad 3.1c$$

$$\frac{d\rho}{du}\frac{du}{ds}\frac{ds}{dt} = \eta[Bn\big(1 - (1 + \epsilon u)\big) - (1 + \epsilon u) - (2(1 + \epsilon u) - 1)E^2 \quad 3.2a$$

$$u'\epsilon^2 = \eta[-Bnu\epsilon - 1 - \epsilon u - (2 - 2\epsilon u + 1)E^2] \quad 3.2b$$

$$u' = \eta\epsilon^{-2}[-Bnu\epsilon - 1 - \epsilon u - (2\epsilon u + 1)E^2] \quad 3.2c$$

$$\frac{dn}{ds}\frac{ds}{dt} = \eta[J - n - 2Bn(1 - (1 + \epsilon u)] \quad 3.3a$$

$$n'\epsilon = \eta[J - n + 2Bn\epsilon u] \quad 3.3b$$

$$n' = \eta\epsilon^{-1}[J - n + 2Bn\epsilon u] \quad 3.3c$$

In the above equations the prime means differentiation with respect to s.

Since $\epsilon^{-2} \gg \epsilon^{-1}\ as\ \epsilon \to 0$, u is faster than n and it could be eliminated adiabatically from equation (3.2c) then $0 = \eta\epsilon^{-2}[-Bnu\epsilon - 1 - \epsilon u - (2\epsilon u + 1)E^2$

$$0 = (-Bn\epsilon - 2\epsilon\, E^2 - \epsilon)u - (1 + E^2)$$

$$u = -\frac{1 + E^2}{Bn\epsilon} \tag{3.4}$$

As mentioned previously the complex electric field is composed of both the real part, which is related to the amplitude, and the imaginary part which is related to the phase, introducing the decomposition:

$$E = R\, e^{i\delta s + i\varphi} \tag{3.5}$$

Take the derivative of E with respect to s, we obtain

$$E' = R'^{e^{i\delta s + i\varphi}} + i(\delta + \varphi')e^{i\delta s + i\varphi} \tag{3.6}$$

Compare equation (3.6) with equation $(3.1c)$ we get

$$R'^{e^{i\delta s + i\varphi}} + i(\delta + \varphi')e^{i\delta s + i\varphi} = \frac{1}{2}(1 + i\alpha)[2u(1 + \epsilon)]E + \gamma e^{i\delta s}] \tag{3.7}$$

Substitute 3.5 and then Divide both side by $e^{i\delta s + i\varphi}$

$$R' + iR(\delta + \varphi') = \frac{1}{2}(1 + i\alpha)[1 + 2u(1 + \epsilon)]R + \gamma e^{-i\varphi}] \tag{3.8}$$

Separate the real parts and the imaginary part we get

$$R' = \frac{1}{2}[1 + 2u(1 + \epsilon)]R + \gamma cos\varphi] \tag{3.8a}$$

$$R(\delta + \varphi') = \frac{1}{2}(\alpha)[1 + 2u(1 + \epsilon)]R - \gamma sin\varphi \tag{3.8b}$$

By substituting equation (3.4)

$$R' = \frac{1}{2}\left[1 + \frac{2\left(-(1+E^2)\right)}{Bn\epsilon}(1+\epsilon)\right]R + \gamma cos\varphi \quad \text{3.8aa}$$

$$(\delta + \varphi')R = \frac{1}{2}(\alpha)\left[1 + \frac{2\left(-(1+E^2)\right)}{Bn\epsilon}(1+\epsilon)\right]R - \gamma sin\varphi \quad \text{3.8ba}$$

Taking the limit $\epsilon \to 0$ and substituting $E^2 = R^2$ from equation (3.5)

$$R' = \frac{1}{2}\left[1 - \frac{2(1+R^2)}{Bn\epsilon}\right]R + \gamma cos\varphi \quad \text{3.8ab}$$

$$\varphi' = -\delta + \frac{1}{2}(\alpha)\left[1 - \frac{2(1+R^2)}{Bn\epsilon}\right] - \frac{\gamma sin\varphi}{R} \quad \text{3.8bb}$$

Also substitute equation (3.4) in equation (3.3d)

$$n' = \eta\epsilon^{-1}\left[J - n + 2Bn\epsilon\left(-\frac{1+R^2}{Bn\epsilon}\right)\right] \quad \text{3.8e}$$

$$n' = \eta\epsilon^{-1}[J - n - 2(1+R^2)] \quad \text{3.8f}$$

3.1.2 Steady state solution

At steady state $n',\ R' and\ \varphi' a$ are all zero

Substitute in (3.8f) for $n' = 0$

$$J - n_s - 2(1+R^2) = 0$$

$$n_s = J - 2(1+R^2) \quad \text{3.8g}$$

Subscript s here means at steady state.

Also substitute in equation (3.8ab) for $R' = 0$, we get

$$\frac{1}{2}\left[1-\frac{2(1+R^2)}{Bn_S\epsilon}\right]R_s=(\gamma cos\varphi)_s \quad 3.8ac$$

Introducing

$$F=\frac{1}{2}\left[1-\frac{2(1+R_s^2)}{B\epsilon(J-2(1+R_s^2)}\right] \quad 3.9$$

Then (3.8ac) become

$$FR_s=(\gamma cos\varphi)_s \quad 3.8ad$$

If $\gamma=0$, we find the laser threshold at $J=J_{th}$, where

$$J_{th}=2+2/B\epsilon \quad 3.8ae$$

Finally, for $\varphi'=0$

$$\left(-\delta+\frac{1}{2}(\alpha)\left[1-\frac{2(1+R_s^2)}{Bn_S\epsilon}\right]\right)R_s=(\gamma sin\varphi)_s \quad 3.8bc$$

$$(-\delta+\alpha F)R_s=(\gamma sin\varphi)_s \quad 3.8bd$$

By taking the square of both sides of (3.8ad) and (3.8bd) and adding them we find

$$F^2R_s^2+(-\delta+\alpha F)^2R_s^2=\gamma^2(sin\varphi^2+cos\varphi^2) \quad 3.10a$$

$$(F^2+(-\delta+\alpha F)^2)R_s^2=\gamma^2 \quad 3.10b$$

In order to form the jacobian matrix, we need to take the partial derivative of $R', \varphi'$and $n'$for each variable state R, φ and n. According to the equations (3.8a), (3.8b) and (3.8f)

$$\frac{dR'}{dR}=\frac{1}{2}\left[1-\frac{2(1+R_s^2)}{Bn\epsilon}\right]-\frac{2R_s^2}{Bn\epsilon} \quad 3.11a$$

$$\frac{dR'}{d\varphi} = -\gamma sin\varphi = (\delta - \alpha F)R_s \tag{3.11b}$$

$$\frac{dR'}{dn} = \frac{(1+R_s^2)}{B\epsilon n^2} R_s \tag{3.11c}$$

$$\frac{d\varphi'}{dR} = \frac{-2(\alpha)R_s}{Bn\epsilon} + \frac{\gamma sin\varphi}{R_s^2} = \frac{-2(\alpha)R_s}{Bn\epsilon} + \left(\frac{-\delta + \alpha F}{R_s}\right) \tag{3.12a}$$

$$\frac{d\varphi'}{d\varphi} = -\frac{\gamma cos\varphi}{R_s} = -\frac{FR_s}{R_s} = -F \tag{3.12b}$$

$$\frac{d\varphi'}{dn} = \frac{(1+R_s^2)}{B\epsilon n^2}\alpha \tag{3.12c}$$

$$\frac{dn'}{dR} = -4\eta\epsilon^{-1}R_s \tag{3.13a}$$

$$\frac{dn'}{d\varphi} = 0 \tag{3.13b}$$

$$\frac{dn'}{dn} = -\eta\epsilon^{-1} \tag{3.13c}$$

For simplicity we introduce

$$G = \frac{1}{2}\left(1 - \frac{2(1+3R_s^2)}{B\epsilon\left(J - 2(1+R_s^2)\right)}\right) \tag{3.14a}$$

$$F - G = \frac{1}{2}\left[1 - \frac{2(1+R_s^2)}{B\epsilon(J - 2(1+R_s^2)}\right] - \frac{1}{2}\left(1 - \frac{2(1+3R_s^2)}{B\epsilon\left(J - 2(1+R_s^2)\right)}\right)$$

$$= \frac{2R_s^2}{B\epsilon\left(J - 2(1+R_s^2)\right)} \tag{3.14b}$$

$$G + F = \frac{1}{2}\left(1 - \frac{2(1+3R_s^2)}{B\epsilon\left(J - 2(1+R_s^2)\right)}\right) + \frac{1}{2}\left[1 - \frac{2(1+R_s^2)}{B\epsilon(J-2(1+R_s^2)}\right]$$

$$= 1 - \frac{(2+4R_s^2)}{B\epsilon(J-2(1+R_s^2)} \qquad 3.14c$$

$$1 - 2F = 1 - 2\frac{1}{2}\left[1 - \frac{2(1+R_s\ ^2)}{B\epsilon(J-2(1+R^2)}\right] = \frac{2(1+R_s^2)}{B\epsilon(J-2(1+R_s^2)} \qquad 3.14d$$

By comparing equation (3.11a) with (3.14a) we get:

$$\frac{dR'}{dR} = G \qquad 3.11a'$$

Also, by substituting equation (3.14d) in (3.11c) we get:

$$\frac{dR'}{dn} = \frac{\frac{1}{2}(1-2F)R_s}{n} \qquad 3.11c'$$

$$\frac{d\varphi'}{dn} = \frac{\frac{1}{2}(1-2F)}{n}\alpha \qquad 3.12c'$$

The Jacobian matrix become:

$$\begin{bmatrix} G-\sigma & (\delta-\alpha F)R_s & \frac{\frac{1}{2}(1-2F)R_s}{n_s} \\ \frac{-2(\alpha)R_s}{Bn_s\epsilon} + (\frac{-\delta+\alpha F}{R_s}) & -F-\sigma & \frac{\frac{1}{2}(1-2F)}{n_s}\alpha \\ -4\eta\epsilon^{-1}R_s & 0 & -\eta\epsilon^{-1}-\sigma \end{bmatrix} \qquad 3.13$$

To find the solution, the determinant of the jacobian matrix equate to zero

$$0 = (G-\sigma)[(-F-\sigma)(-\eta\epsilon^{-1}-\sigma) - 0\,]$$

$$-(\delta-\alpha F)R_s\left[\left\{-\frac{2R_s}{B\epsilon n_s}\alpha+\left(\frac{-\delta+\alpha F}{R_s}\right)\right\}\{-\eta\epsilon^{-1}-\sigma\}\right.$$

$$\left.+\frac{\frac{1}{2}(1-2F)}{n}\alpha 4\eta\epsilon^{-1}R_s\right]$$

$$+\frac{\frac{1}{2}(1-2F)R_s}{n_s}[(-F-\sigma)(4\eta\epsilon^{-1}R_s)] = a+b+c \qquad 3.13a$$

Where a, b and c as follow:

$$a = (G-\sigma)[F\eta\epsilon^{-1}+F\sigma+\sigma\,\eta\epsilon^{-1}+\sigma^2]$$

$$a = GF\eta\epsilon^{-1}+FG\sigma+G\sigma\,\eta\epsilon^{-1}+G\sigma^2-F\eta\epsilon^{-1}\sigma-F\sigma^2-\sigma^2\,\eta\epsilon^{-1}-\sigma^3$$

$$a = \sigma^3-(G-F-\eta\epsilon^{-1})\sigma^2-(FG+G\eta\epsilon^{-1}-F\eta\epsilon^{-1})\sigma-GF\eta\epsilon^{-1} \qquad 3.14$$

$$b = -(\delta-\alpha F)R_s\left[\frac{2R_s}{B\epsilon n_s}\alpha\eta\epsilon^{-1}+\frac{2R_s}{B\epsilon n}\alpha\sigma-\left(\frac{-\delta+\alpha F}{R_s}\right)\eta\epsilon^{-1}-\left(\frac{-\delta+\alpha F}{R_s}\right)\sigma\right.$$

$$\left.+\frac{\frac{1}{2}(1-2F)}{n_s}\alpha 4\eta\epsilon^{-1}R_s\right]$$

$$b = -(\delta-\alpha F)\alpha(F-G)\eta\epsilon^{-1}-(\delta-\alpha F)\alpha(F-G)\sigma-(\delta-\alpha F)^2\eta\epsilon^{-1}$$

$$-(\delta-\alpha F)^2\sigma-(\delta-\alpha F){R_s}^2\frac{(1-2F)}{n}2\alpha\eta\epsilon^{-1}$$

$$b = \left((\delta - \alpha F)\alpha(F - G) + (\delta - \alpha F)^2\right)\sigma + \left((\delta - \alpha F)\alpha(F - G) + (\delta - \alpha F)^2\right)\eta\epsilon^{-1} + (\delta - \alpha F)(1 - 2F)(F - G)\alpha B\eta \quad 3.15$$

$$c = -\frac{2(1 - 2F){R_s}^2\alpha}{\left(J - 2\left(1 + {R_s}^2\right)\right)}F\eta\epsilon^{-1} - \frac{2(1 - 2F){R_s}^2\alpha}{\left(J - 2\left(1 + {R_s}^2\right)\right)}\sigma\eta\epsilon^{-1}$$

$$c = \frac{2(1 - 2F){R_s}^2}{\left(J - 2\left(1 + {R_s}^2\right)\right)}F\eta\epsilon^{-1} + \frac{2(1 - 2F){R_s}^2}{\left(J - 2\left(1 + {R_s}^2\right)\right)}\sigma\eta\epsilon^{-1}$$

$$c = (1 - 2F)F(F - G)B\eta + (1 - 2F)(F - G)B\sigma\eta \quad 3.16$$

From the determinant of the jacobian matrix, we then formulate the characteristic equation for the growth rate, which is given as [78]:

$$\sigma^3 + a_1\sigma^2 + a_2\sigma + a_3 = 0 \quad 3.17$$

Where:

$$a_1 = -(G - F - \eta\epsilon^{-1}) \quad 3.18$$

$$a_2 = -(FG + G\eta\epsilon^{-1} - F\eta\epsilon^{-1}) + \left((\delta - \alpha F)\alpha(F - G) + (\delta - \alpha F)^2\right) + (1 - 2F)(F - G)B\eta \quad 3.19$$

$$a_3 = -GF\eta\epsilon^{-1} + \left((\delta - \alpha F)\alpha(F - G) + (\delta - \alpha F)^2\right)\eta\epsilon^{-1} + (1 - 2F)(F - G)\left((\delta - \alpha F)\alpha + F\right)B\eta \quad 3.20$$

Let

$$\sigma = \eta^{\frac{1}{2}}\lambda_0 + \eta\lambda_1 + \cdots \tag{3.21}$$

Where $\lambda_0$and $\lambda_1$are eigen values

$$\sigma \approx \eta^{\frac{1}{2}}\lambda_0 + \eta\lambda_1 \tag{3.22}$$

$$\sigma^2 = \eta\lambda_0^2 + \eta^2\lambda_1^2 + 2\lambda_0\lambda_1\eta^{\frac{3}{2}} \tag{3.23}$$

$$\sigma^3 = \lambda_0^3\eta^{\frac{3}{2}} + 3\lambda_0\lambda_1^2\eta^{\frac{5}{2}} + 3\lambda_0^2\lambda_1\eta^2 + \lambda_1^3\eta^3 \tag{3.24}$$

$$a_1\sigma^2 = -(G - F - \eta\epsilon^{-1})\left(\eta\lambda_0^2 + \eta^2\lambda_1^2 + 2\lambda_0\lambda_1\eta^{\frac{3}{2}}\right)$$

$$a_1\sigma^2 = (F-G)\eta\lambda_0^2 + (F-G)\eta^2\lambda_1^2 + (F-G)2\lambda_0\lambda_1\eta^{\frac{3}{2}} + \eta^2\lambda_0^2\epsilon^{-1} + \eta^3\lambda_1^2\epsilon^{-1} \quad + 2\lambda_0\lambda_1\eta^{\frac{5}{2}}\epsilon^{-1} \tag{3.25}$$

$$a_2\sigma = \left[-(FG + (G-F)\eta\epsilon^{-1}) + \left((\delta - \alpha F)\alpha(F-G) + (\delta - \alpha F)^2\right) + (1-2F)(F-G)B\eta\right]\left(\eta^{\frac{1}{2}}\lambda_0 + \eta\lambda_1\right)$$

$$a_2\sigma = -FG\eta^{\frac{1}{2}}\lambda_0 - FG\eta\lambda_1 - (G-F)\epsilon^{-1}\eta^{\frac{3}{2}}\lambda_0 - (G-F)\epsilon^{-1}\eta^2\lambda_1 + \left((\delta - \alpha F)\alpha(F-G) + (\delta - \alpha F)^2\right)\eta^{\frac{1}{2}}\lambda_0 + \left((\delta - \alpha F)\alpha(F-G) + (\delta - \alpha F)^2\right)\eta\lambda_1 + (1-2F)(F-G)B\eta^{\frac{3}{2}}\lambda_0 + (1-2F)(F-G)B\eta^2\lambda_1 \tag{3.26}$$

Then the equation (3.13a) becomes

$$\lambda_0^3\eta^{\frac{3}{2}} + 3\lambda_0\lambda_1^2\eta^{\frac{5}{2}} + 3\lambda_0^2\lambda_1\eta^2 + \lambda_1^3\eta^3 + (F-G)\eta\lambda_0^2 + (F-G)\eta^2\lambda_1^2$$
$$+ (F-G)2\lambda_0\lambda_1\eta^{\frac{3}{2}} + \eta^2\lambda_0^2\epsilon^{-1} + \eta^3\lambda_1^2\epsilon^{-1} + 2\lambda_0\lambda_1\eta^{\frac{5}{2}}\epsilon^{-1}$$
$$+ -FG\eta^{\frac{1}{2}}\lambda_0 - FG\eta\lambda_1 - (G-F)\epsilon^{-1}\eta^{\frac{3}{2}}\lambda_0$$
$$- (G-F)\epsilon^{-1}\eta^2\lambda_1$$
$$+ \big((\delta-\alpha F)\alpha(F-G) + (\delta-\alpha F)^2\big)\eta^{\frac{1}{2}}\lambda_0$$
$$+ \big((\delta-\alpha F)\alpha(F-G) + (\delta-\alpha F)^2\big)\eta\lambda_1$$
$$+ (1-2F)(F-G)B\eta^{\frac{3}{2}}\lambda_0 + (1-2F)(F-G)B\eta^2\lambda_1$$
$$+ -GF\eta\epsilon^{-1} + \big((\delta-\alpha F)\alpha(F-G) + (\delta-\alpha F)^2\big)\eta\epsilon^{-1}$$
$$+ (1-2F)(F-G)\big((\delta-\alpha F)\alpha + F\big)B\eta = 0 \qquad 3.27$$

Gathering the coefficient of each power of $\eta^3, \eta^{\frac{5}{2}}, \eta^2, \eta^{\frac{3}{2}}, \eta \; and \; \eta^{\frac{1}{2}}$

$$
\begin{aligned}
&(\lambda_1^3 + \lambda_1^2\epsilon^{-1})\,\eta^3 + (3\lambda_0\lambda_1^2 + 2\lambda_0\lambda_1\epsilon^{-1})\eta^{\frac{5}{2}} \\
&\quad + (3\lambda_0^2\lambda_1 + (F-G)\lambda_1^2 + \lambda_0^2\epsilon^{-1} - (G-F)\epsilon^{-1}\lambda_1 \\
&\quad + (1-2F)(F-G)B\lambda_1)\eta^2 \\
&\quad + (\,(F-G)2\lambda_0\lambda_1 + \lambda_0^3 - (G-F)\epsilon^{-1}\,\lambda_0 \\
&\quad + (1-2F)(F-G)B\lambda_0)\eta^{\frac{3}{2}} \\
&\quad + \Big((F-G)\lambda_0^2 - FG\lambda_1 \\
&\quad + \big((\delta-\alpha F)\alpha(F-G) + (\delta-\alpha F)^2\big)\lambda_1 - GF\epsilon^{-1} \\
&\quad + \big((\delta-\alpha F)\alpha(F-G) + (\delta-\alpha F)^2\big)\epsilon^{-1} \\
&\quad + (1-2F)(F-G)\big((\delta-\alpha F)\alpha + F\big)B\Big)\,\eta \\
&\quad + \big(-FG\,\lambda_0 + \big((\delta-\alpha F)\alpha(F-G) + (\delta-\alpha F)^2\big)\lambda_0\,\big)\eta^{\frac{1}{2}} \\
&\quad = 0
\end{aligned}
\qquad 3.28
$$

After that, we equate the coefficient of each power to zero,

For η^3 and $\eta^{\frac{5}{2}}$

$$\lambda_1^2(\lambda_1 + \epsilon^{-1}) = 0\ then\ \lambda_1 = 0\ or - \epsilon^{-1} \qquad 3.28a$$

$$3\lambda_0\lambda_1^2 + 2\lambda_0\lambda_1\epsilon^{-1} = 0, \lambda_0 = 0\ or\ \lambda_1 = -\frac{2}{3} \qquad 3.28b$$

Both of the previous equations give trivial solutions.

For η^2

$$3\lambda_0^2\lambda_1 + (F-G)\lambda_1^2 + \lambda_0^2\epsilon^{-1} - (G-F)\epsilon^{-1}\lambda_1 + (1-2F)(F-G)B\lambda_1 = 0$$

$$\lambda_0^2(3\lambda_1 + \epsilon^{-1}) + (F-G)\lambda_1^2 + \left((1-2F)(F-G)B - (G-F)\epsilon^{-1}\right)\lambda_1 = 0$$

$$\lambda_0^2 = -\frac{(F-G)\lambda_1^2 + \left((1-2F)(F-G)B - (G-F)\epsilon^{-1}\right)\lambda_1}{(3\lambda_1 + \epsilon^{-1})} \qquad 3.28c$$

For $\eta^{\frac{3}{2}}$

$$(F-G)2\lambda_0\lambda_1 + \lambda_0^3 - (G-F)\epsilon^{-1}\lambda_0 + (1-2F)(F-G)B\lambda_0 = 0$$

$$\lambda_0(\lambda_0^2 + (F-G)2\lambda_1 - (G-F)\epsilon^{-1} + (1-2F)(F-G)B) = 0$$

Then

$$\lambda_0 = 0 \; or \; \lambda_0^2 + (F-G)(2\lambda_1 + \epsilon^{-1} + (1-2F)B)$$

$$\lambda_0^2 = -(F-G)(2\lambda_1 + \epsilon^{-1} + (1-2F)B) \qquad 3.28d$$

Equate two equations (2.28c) and (2.28d)

$$(F-G)\lambda_1^2 + \left((1-2F)(F-G)B - (G-F)\epsilon^{-1}\right)\lambda_1 = (3\lambda_1 + \epsilon^{-1})(F-G)(2\lambda_1 + \epsilon^{-1} + (1-2F)B)$$

$$\lambda_1^2 + \left((1-2F)B + \epsilon^{-1}\right)\lambda_1 = 6\lambda_1^2 + 3(\epsilon^{-1} + (1-2F)B) + 2\epsilon^{-1})\lambda_1 + \epsilon^{-1}(\epsilon^{-1} + (1-2F)B)$$

$$5\lambda_1^2 - (2(1-2F)B - 4\epsilon^{-1})\lambda_1 - \epsilon^{-1}(\epsilon^{-1} + (1-2F)B) = 0$$

We find an expression for λ_1

$$\lambda_1 = \frac{(1-2F)B - 2\epsilon^{-1}}{5} \pm \frac{1}{5}\sqrt{((1-2F)B - 2\epsilon^{-1})^2 - 5\epsilon^{-1}(\epsilon^{-1} + (1-2F)B)} \quad 3.28e$$

Substitute in equation (3.28d)

$$\lambda_0 = \pm i\sqrt{\frac{}{(F-G)}\left(2\frac{(1-2F)B - 2\epsilon^{-1}}{5} \pm \frac{2}{5}\sqrt{((1-2F)B - 2\epsilon^{-1})^2 - 5\epsilon^{-1}(\epsilon^{-1} + (1-2F)B)} + \epsilon^{-1} + (1-2F)B\right)} \quad 3.28f$$

Equate the factor of $\eta^{\frac{1}{2}}$ to zero yields that

$$\left(-FG\,\lambda_0 + \left((\delta - \alpha F)\alpha(F-G) + (\delta - \alpha F)^2\right)\lambda_0\right) = 0$$

Then $\lambda_0 = 0$ which is trivial solution or

$$FG = \left((\delta - \alpha F)\alpha(F-G) + (\delta - \alpha F)^2\right) \quad 3.28g$$

Also, equate the factor of η to zero and substitute equation (3.28g) leads to:

$$\left((F-G)\lambda_0^2+(1-2F)(F-G)\big((\delta-\alpha F)\alpha+F\big)B\right)=0 \qquad 3.28h$$

$$\lambda_0^2=-((1-2F)\big((\delta-\alpha F)\alpha+F\big)B \qquad 3.28i$$

$$\lambda_0=\pm i\sqrt{(1-2F)B((\delta-\alpha F)\alpha+F)} \qquad 3.28j$$

According to equation (3.28d):

$$\lambda_1=\frac{(1-2F)\big((\delta-\alpha F)\alpha+F\big)B}{2(F-G)}+\frac{1}{2}(\epsilon^{-1}+(1-2F)B) \qquad 3.28K$$

Then, according to equation (3.22)

$$\sigma_1\approx\ \pm i\sqrt{(F-G)\left(2\frac{(1-2F)B-2\epsilon^{-1}}{5}\pm\frac{2}{5}\sqrt{((1-2F)B-2\epsilon^{-1})^2-5\epsilon^{-1}\big(\epsilon^{-1}+(1-2F)B\big)}+\epsilon^{-1}+(1-2F)B\right)}\eta$$

$$+\left(\frac{(1-2F)B-2\epsilon^{-1}}{5}\right. \qquad 3.29$$

$$\left.\pm\frac{1}{5}\sqrt{((1-2F)B-2\epsilon^{-1})^2-5\epsilon^{-1}(\epsilon^{-1}+(1-2F)B)}\ \right)\eta$$

The imaginary part of expression (3.28f) gives the RO frequency

ω_{RO} 3.29a

$$= \pm \sqrt{\left(\frac{2}{5}\sqrt{((1-2F)B-2\epsilon^{-1})^2 - 5\epsilon^{-1}(\epsilon^{-1}+(1-2F)B)} + \epsilon^{-1} + (1-2F)B \right) \eta}$$

The real part of expression (3.29) gives the damping rate (r_{RO})

$$\Gamma_{RO} = \left(\frac{(1-2F)B-2\epsilon^{-1}}{5} \pm \frac{1}{5}\sqrt{((1-2F)B-2\epsilon^{-1})^2 - 5\epsilon^{-1}(\epsilon^{-1}+(1-2F)B)}\right)\eta \quad 2.29b$$

Also,

$$\sigma_2 \approx \pm i\sqrt{(1-2F)B\big((\delta-\alpha F)\alpha+F\big)\eta} + \left(\frac{(1-2F)\big((\delta-\alpha F)\alpha+F\big)B}{2(F-G)} + \frac{1}{2}(\epsilon^{-1} + (1-2F)B)\right)\eta \quad 2.30$$

Where

$$\omega_{RO2} = \pm\sqrt{(1-2F)B\big((\delta-\alpha F)\alpha+F\big)\eta} \quad 2.30a$$

$$\Gamma_{RO2} = \left(\frac{(1-2F)\big((\delta-\alpha F)\alpha+F\big)B}{2(F-G)} + \frac{1}{2}(\epsilon^{-1}+(1-2F)B)\right)\eta \qquad 2.30b$$

3.2 Computational Steps

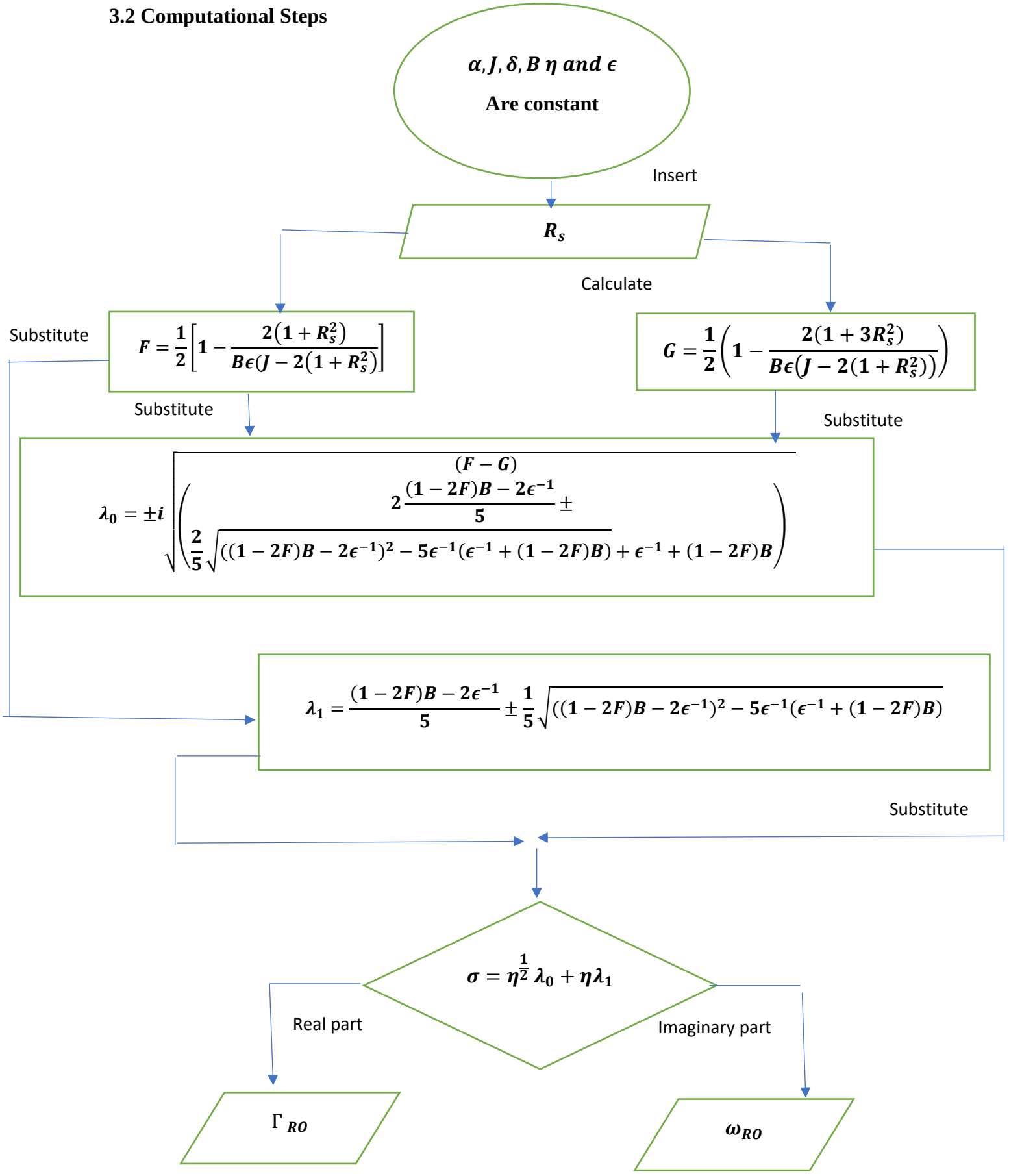

3.3 Numerical Results

3.3.1 Dynamic Response of QDLs to Optical feedback

In order to investigate our results, we will examine the response of QDL of a five-layer structure grown by solid-source MBE to optical feedback. This QDL consist of 2.4 InAs monolayers topped with 5 nm GaInAs stacked in a 400 nm thick optical cavity. A GaAs spacer of 35 nm is also used between the QD layers. We discuss its dynamics by using the following constants shown in table 3.1 below, which were also utilized by Thomas Eraneux [82].

Table 3.1: Physical parameters used in the simulation of the QDL model unless stated otherwise.

Parameters	Value
g	1.01
ϵ	0.01
B	10^2
J_{th}	4
α	1.2
η	2×10^{-3}

`

We characterize the dynamics of QDL subjected to the optical feedback that operate above threshold region $J => J_{th}$. The control parameters that are varied are the detuning frequency and the injection rate. The injection rate for both negative and positive detuning frequency is

plotted versus R_S in figure 3.1 (a) and (b), respectively. It is noticeable that, for all negative detuning frequencies there exist two or more different R_S with the same injection rate and the same detuning frequency. While for positive detuning there is only one R_S except for ($\delta = 0.1$). This phenomena was also reported in literature data [83]. Except this region, for all detuning frequencies raising the injection rate drastically increases the steady state intensity related quantity R_s. Increasing the injection rate indicates that a large portion of light is generated and trapped within the active layer rather than escaping to the surrounding via scattering or absorption, which improves the gain, reduces optical losses, and boots steady state intensity. Additionally, for positive detuning frequency, the injection rate is larger for larger δ, which means a large injection rate needed in order to reach the steady state intensity as the detuning frequency increased.

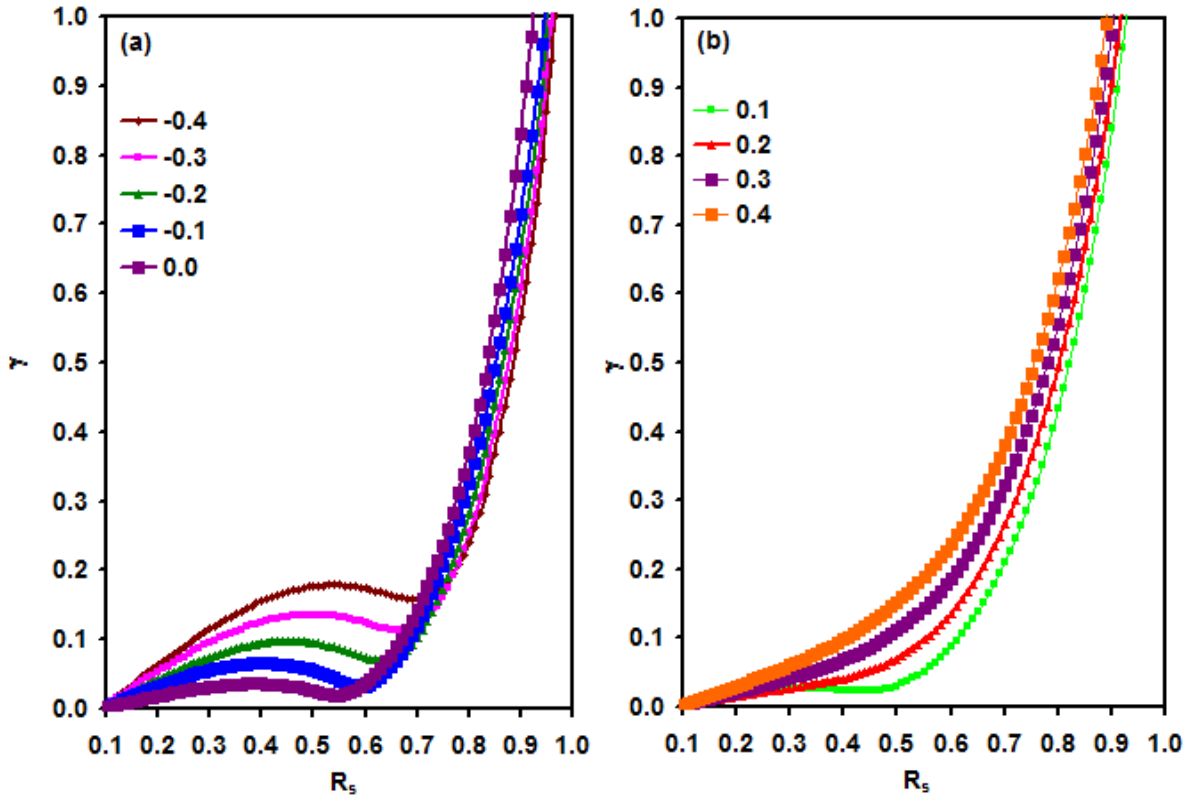

Figure 3.1: injection rate γ versus R_S for (a): negative detuning δ, and (b): positive detuning δ.

To visualize the effect of changing injection rate in the dynamics of the system, we manipulate two cases one for negative ($\delta = -0.4$) and other for positive (δ = 0.4) detuning frequency by varying the injection rate up to (1). For each negative and positive detuning frequencies, the RO frequency increase and the damping rate decrease as illustrated in figures 3.2 (a), 3.2 (b), 3.3 and 3.4. This implies that further increasing of the injection rate, the system tends toward instability and chaotic behavior. In both cases, the solution gives a negative damping rate for low injection rate, which implies the stability of the system [84]. Further increasing of injection rate, the damping rate becomes positive and so the system goes to instabilities. It is worth noting that for (δ = 0.4) the system exhibts stability over a wide range of injection rate than ($\delta = -0.4$). In the case of ($\delta = -0.4$), different values of both damping rate and relaxation oscillation for the same injection rate in the inset of figure 3.3 and 3.4 indicates the appearance of bistabilty or excitability. While it is absent for ($\delta =$ 0.4). Bistabillity means the ability of the system to operate at two stable states with different intensities [85], which enables the system to transit from one state to another at specific conditions. This provide the opportunities for control and manipulation the laser output which can be utilized in various optical technologies such as optical switching [86] and optical memory.

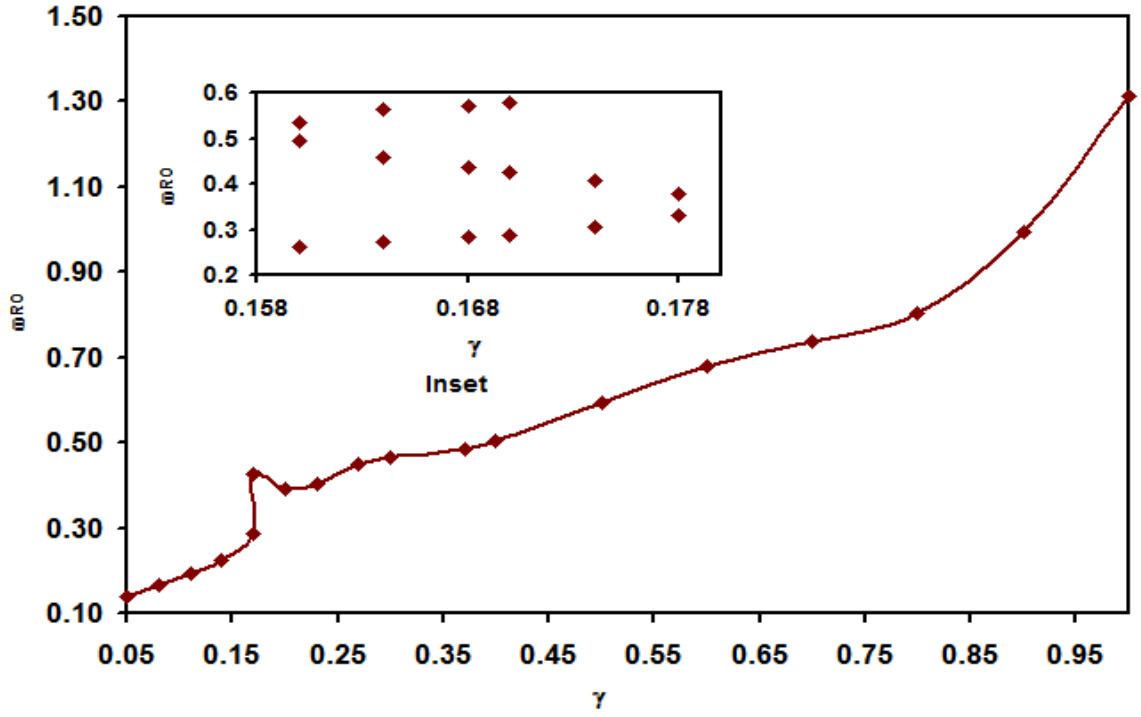

Figure 3.2: RO frequency ω_{RO} versus injection rate γ for $\delta = -0.4$. The inset represent different value of RO frequency ω_{RO} in bistability region.

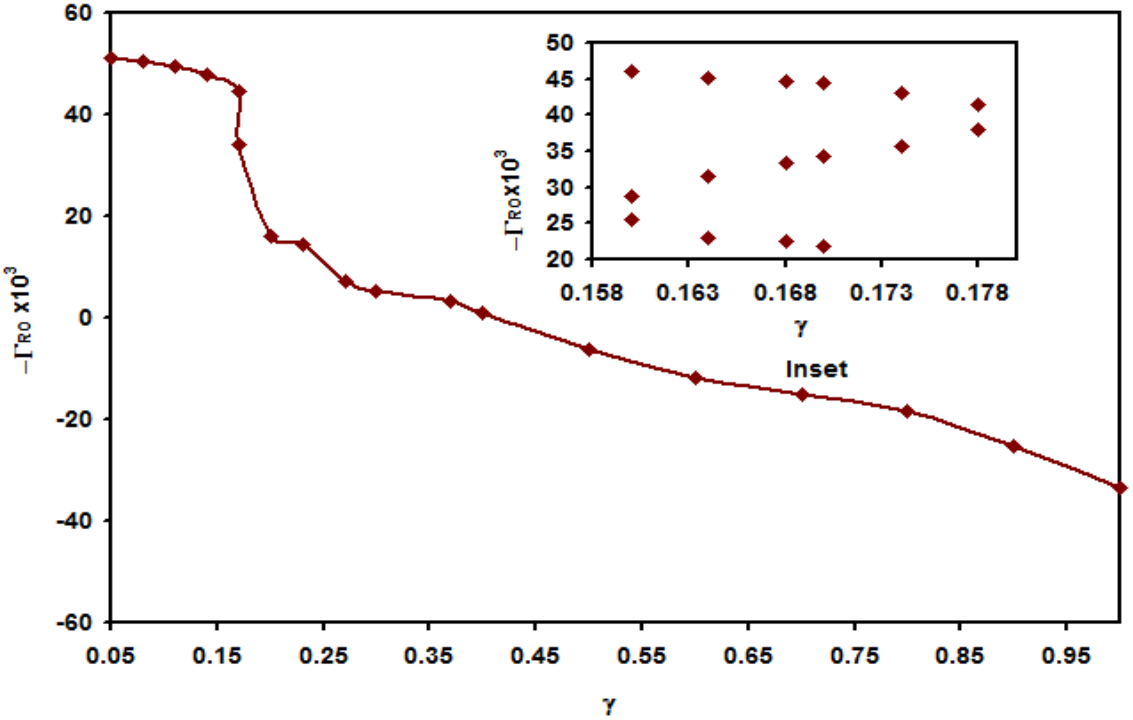

Figure 3.3: Damping rate Γ_{RO} versus injection rate γ for $\delta = -0.4$. The inset represent different value of damping rate Γ_{RO} in bistability region.

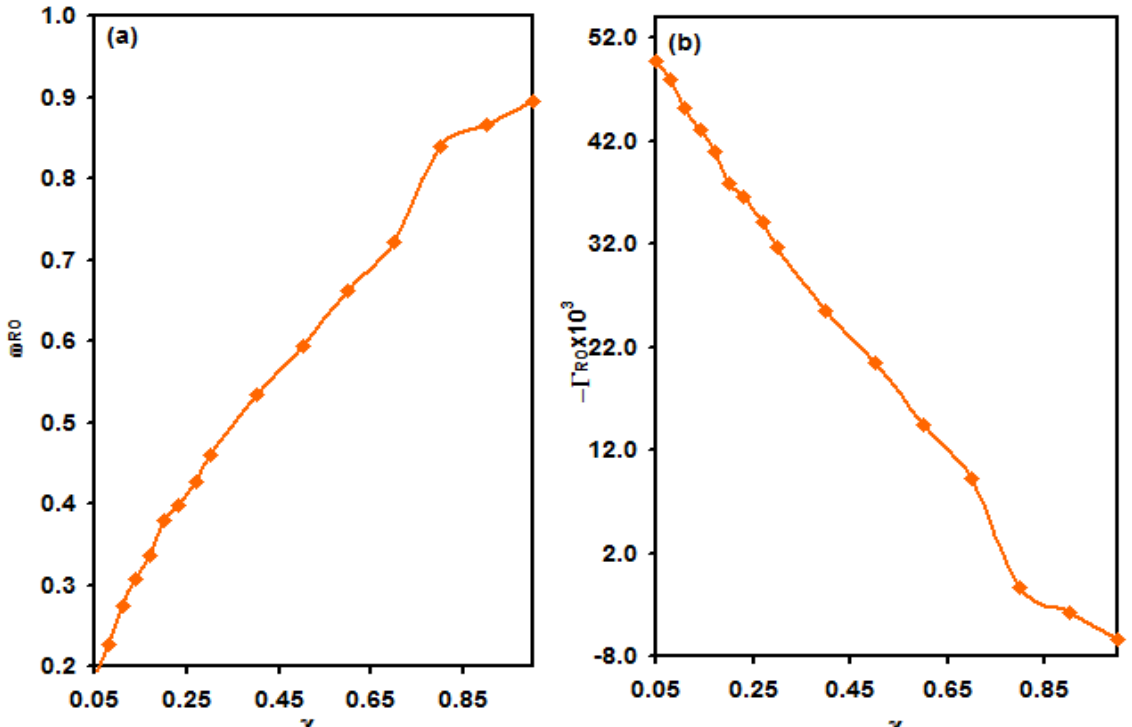

Figure 3.4: (a) RO frequency ω_{RO} versus the injection rate Γ for $\delta = 0.4$ and (b) Damping rate Γ_{RO} versus injection rate γ for $\delta = 0.4$.

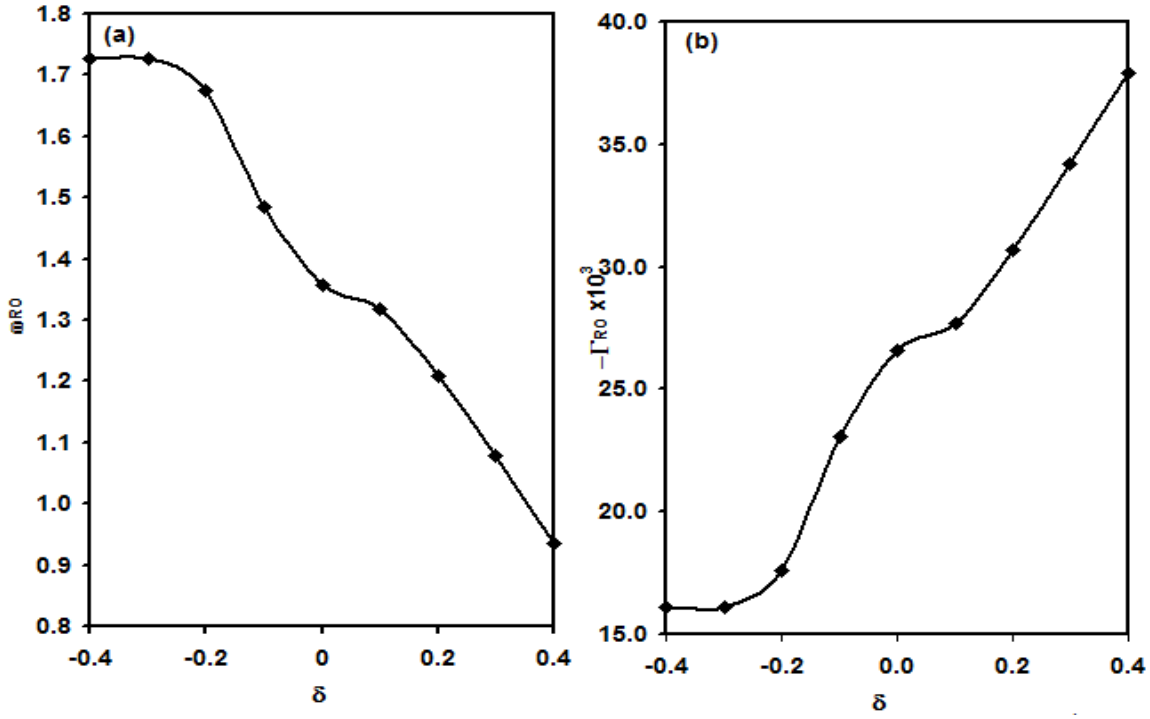

Figure 3.5: (a) RO frequency ω_{RO} versus the detuning frequency δ at constant injection rate γ.And (b) Damping rate Γ_{RO} versus the detuning frequency δ at constant injection rate γ.

At constant injection rate ($\gamma = 0.2$) , the RO frequency and the damping rate are plotted versus the detuning frequency as shown in figures 3.5 (a) and (b) , respectively. Increasing the detuning frequency at constant injection rate has a noticeable effect on the RO frequency and the damping rate. Specifically, as the detuning frequency increases, the RO frequency decreases, and the damping rate increases. This pattern indicates an improvement in the stability of the system.

In this context, the detuning frequency is defined as the difference between the master laser and the slave laser frequencies. In our scenario, this detuning frequency δ corresponds to the difference between the frequency of the laser reflected back into the cavity ω_L and the resonance frequency of the cavityω_0. It's worth noting that the resonance frequency depends upon the cavity length. Consequently, controlling the detuning can be achieved by adjusting the cavity length. Therefore, enhancing stabilization can be accomplished through precision manufacturing processes.

All the previous analysis according to the first solution of the characteristic equation of growth rate σ_1 is presented in equation (3.29). The other solution related to σ_2 when applied to this system reveals unstable solution and shows either regular or irregular oscillations [87] for both negative and positive detuning as presented in figure 3.6 (a). Also, for positive detuning frequency, there is a lack of imaginary parts in the solution which means the system is free from relaxation oscillation as appear in figure 3.6 (b). We will ignore this solution since our aim is to study the stability region of the system. Our next analysis depends on the first solution given by σ_1.

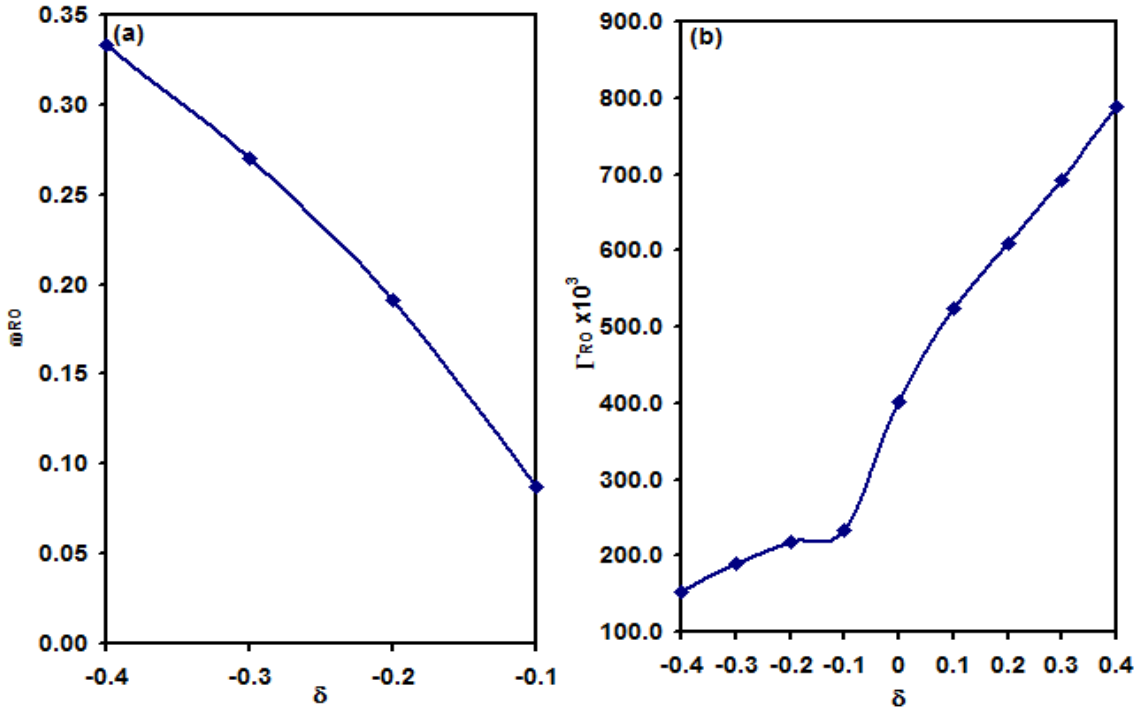

Figure 3.6: (a) RO frequency ω_{RO} versus detuning frequency at constant injection rate $\gamma = 0.2$ according to the second solution of characteristic equation σ_2 and (b) Damping rate Γ_{RO} versus detuning frequency at constant injection rate $\gamma = 0.2$ according to the second solution of characteristic equation σ_2.

3.3.2 Comparison between Dynamics of solitary and subjected to optical feedback QDLs.

In this section we aim to compare the impact of optical feedback on the dynamics of QDLs for one case where ($\delta = -0.4$) with those of solitary QDLs. It is well known that the RO frequency in the presence of optical feedbacks shifts from that of solitary oscillation [87]. However, in our case it takes larger value than that of the solitary oscillation at the same value of steady state intensity as shown in figures 3.7(a). In a stability regime, the damping rate of the oscillations is lower than the damping in the solitary oscillation which indicates that the system is less stable than predicted from solitary model. Moreover, there is an

instability regime indicated by positive damping rate. Furthermore, as explained in previous section, the optical feedback provides bistability phenomena, which provide an ability to use as optical switch.

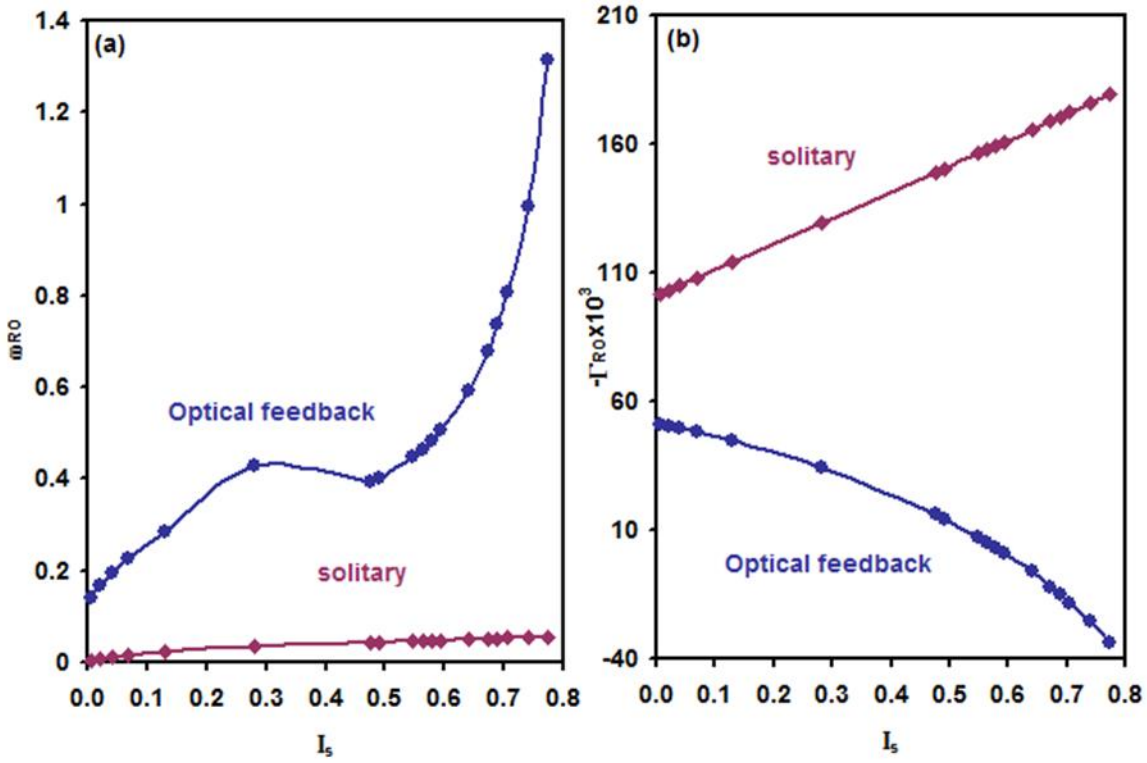

Figure 3.7: (a) RO frequency ω_{RO}versus steady state intensity I_s for solitary and under optical feedback QDL and (b) Damping rate Γ_{RO} versuse steady state intensity I_s for solitary and under optical feedback QDL.

Figures 3.8 (a) and (b) exhibit the damping rate of solitary QDL and in presence of optical feedback (in stability region), respectively, as a function of the squared RO frequency. In both cases, the evolution is linear, following the relationship [88].

$$\Gamma_{RO} = K\,\omega_{RO}^2 + \gamma_0 \qquad 3.29$$

With K as the slope and γ_0 as the inverse of the differential carrier lifetime. For solitary laser the slope is positive which means that as the RO frequency increase the damping rate increase. Consequently, the system become more stable. However, the slope is negative when optical feedback is present, as the RO increase the damping rate decrease. As a result, the system become less stable, leading to more fluctuation or even instabilities. Under optical feedback the K factor lowered from 25.25 to -0.11. The sign and the value of K factor give indication about how the system respons to fluctuation, where the small negative value here represent small destabilization in this region. Understanding and determining the K factor are essential in optimizing the laser performance.

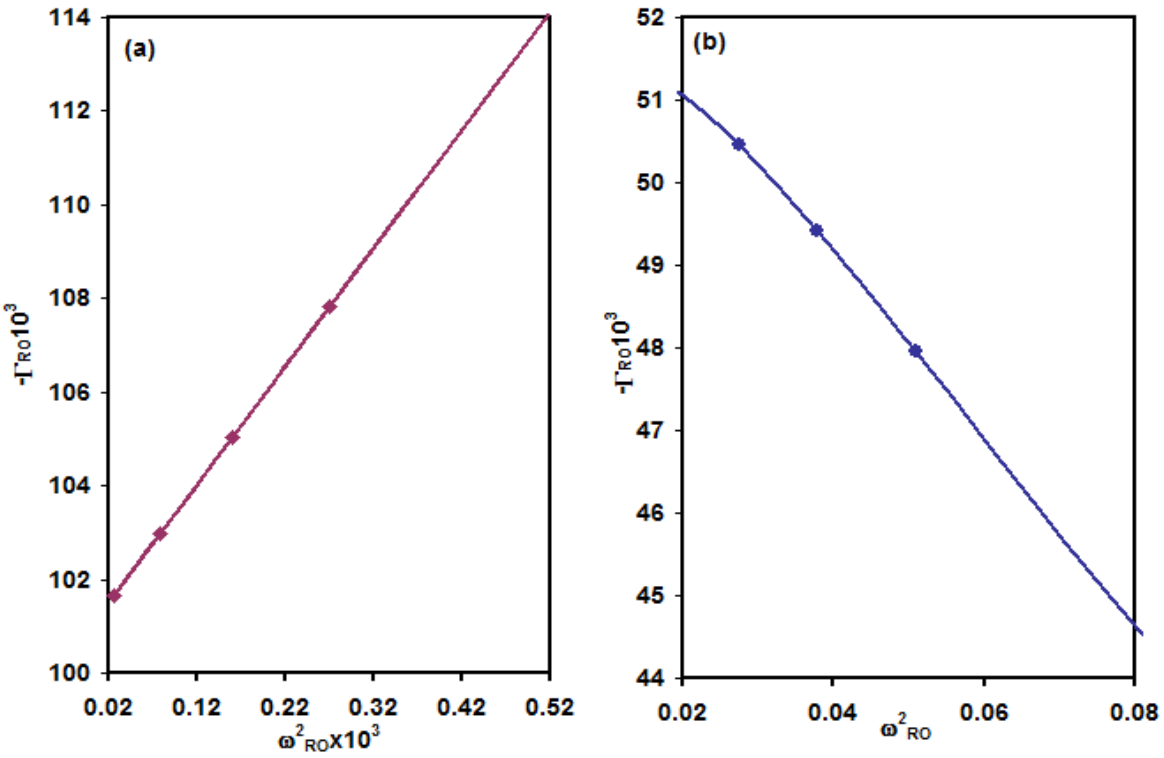

Figure 3.8: Damping rate Γ_{RO} versus the square of RO frequency ω_{RO}^2 for solitary QDL and (b): Damping rate Γ_{RO}versus square of RO frequency ω_{RO}^2QDL under optical feedback.

Chapter 4

Conclusion and Future Work

4.1 Conclusions

In this work, the dynamic response of QDLs subjected to optical feedback was explored analytically utilizing a rate equation model developed by O'Brien et al. An expressions for both the relaxation oscillation and the damping rate were derived analytically in terms of the eigenvalues of the Jacobian matrix evaluated at steady state. Our findings were numerically validated by studying the reaction of a five-layer structure generated by solid-source MBE to optical feedback. The computation revealed that both RO oscillation and damping rate depend on steady state intensity, which in turn depend on carrier rate injection. In addition, the study showed that under optical feedback at constant detuning frequency the RO frequency increased while the damping rate decreased as the injection rate increased. For small injection rate, the system still stable. However, with further increasing of the injection rate the system goes to instabilities and chaotic region. Moreover, for negative detuning frequency, there is bistability region which enables to use the laser in various applications such as optical switch and optical data storing. Comparing to solitary QDLs, the analysis revealed a negative damping factor under optical feedback which indicates a decrease in laser stability.

4.2 **Future work**

We are convinced that scientific advancement in the field of quantum dot laser should be a combination of experimental and theoretical efforts. As a result, we can broaden our study by concentrating on the experimental realization of QDLs response proposed in the

theoretical context. Take in to account the realistic obstacles and constraints while implementing it in real-world. It is also feasible to investigate the dynamic response of QDLs utilizing various materials and structures. Examine how changes in QDs attributes affect overall performance and dynamic behavior.

Looking ahead, the findings of this study offer up new avenues for the employment of quantum dot lasers in emerging technologies. Because of the improved dynamic responsiveness, future work could investigate the usage of QDLs under optical feedback in quantum communication protocols such as quantum key distribution. Examine how dynamic responses affect the security and efficiency of quantum communication operations.

References

Hamdan, A. L., Sataloff, R. T., Ramadan, O., Eichorn, D., & Hawkshaw, M. J. (2023). *Blue Laser Surgery in Laryngology*. Springer Nature.

Yeo, C. Y., Tam, S. C., Jana, S., & Lau, M. W. (1994). A technical review of the laser drilling of aerospace materials. *Journal of materials processing technology*, *42*(1), 15-49.

Biswas, D. J. (2023). *A Beginner's Guide to Lasers and Their Applications, Part 1: Insights into Laser Science*. Springer Nature.

Niemtzow, R. C. (2022). Acupuncture and Lasers. *Medical Acupuncture*, *34*(4), 211-212.

Prasad, R. (2023). Laser Technology and Its Applications. In *Physics and Technology for Engineers: Understanding Materials and Sustainability* (pp. 377-433). Cham: Springer Nature Switzerland.

Liscidini, M., & Sipe, J. E. (2013). Stimulated emission tomography. *Physical review letters*, *111*(19), 193602..

High Efficiency Solar Pumped Laser Through a Ring Array Concentrator - Scientific Figure on ResearchGate. Available from: https://www.researchgate.net/figure/Absorption-spontaneous-emission-and-stimulated-emission-17_fig2_322861305 [accessed 16 Jan, 2024].

http://lorenzosworld.com/bachelor.html [accessed 16 Jan, 2024]

Kannatey-Asibu Jr, E. (2023). *Principles of Laser Materials Processing: Developments and Applications*. John Wiley & Sons.

Qin, J., Tang, Y., Zhang, J., Shen, T., Karlsson, M., Zhang, T., ... & Gao, F. (2023). From optical pumping to electrical pumping: the threshold overestimation in metal halide perovskites. *Materials Horizons*, *10*(4), 1446-1453.

Inoue, I., Inubushi, Y., Sato, T., Tono, K., Katayama, T., Kameshima, T., ... & Yabashi, M. (2016). Observation of femtosecond X-ray interactions with matter using an X-ray–X-ray pump–probe scheme. *Proceedings of the National Academy of Sciences*, *113*(6), 1492-1497.

Petrova, T. B., Wolford, M. F., Myers, M. C., & Obenschain, S. P. (2023). Modeling of the NRL Electra Electron-Beam Pumped Argon Fluoride Laser. *IEEE Transactions on Plasma Science*.

Smith, J. H., & Robinson, D. W. (1981). Chemical pumping of pure rotational HF lasers. *The Journal of Chemical Physics*, *74*(9), 5111-5115.

Kenneth R. Spring, Thomas J. Fellers and Michael W. Davidson http://www.olympusconfocal.com/theory/laserintro.html,[16 Jan,2024]

AKIL, A. Z. (2023). WORKING PRINCIPLES AND TYPES OF LASERS. *New Technologies and Techniques in Gynecology and Obstetrics*, 15.

Tian, S., Zhang, L., Xie, R., Lu, A., Huang, Y., Xing, H., & Chen, X. (2023). The electronic, magnetic and optical properties of GaN monolayer doped with rare-earth elements. *Solid State Communications*, *371*, 115292.

Sari, N., Salim, F., Sara, M., Fitri, E. W., & Bulqiah, M. (2023). Efficacy of 1064nm neodymium-doped yttrium aluminum garnet (Nd: YAG) laser and 2940nm fractional erbium laser for severe acne with acne scar: a case report. *Bali Medical Journal*, *12*(2), 1676-1679.

F.T Arecchi, instabilities and chaos in quntum optics,spriger ,volume34,1987,page 17. Arecchi, F. T. (1987). Instabilities and chaos in single-mode homogeneous line lasers. In *Instabilities and chaos in quantum optics* (pp. 9-48). Berlin, Heidelberg: Springer Berlin Heidelberg.

Kuwashima, F. K. F., Ichikawa, T. I. T., Kitazima, I. K. I., & Iwasawa, H. I. H. (1999). Chaotic Oscillation in a Single-Mode Class A He–Ne Laser (6328 Å) II. *Japanese journal of applied physics*, *38*(11R), 6321.

Jahanpanah, J., & Rahdar, A. A. (2012). Theory of gain and mode locking in free-running class-B lasers with simultaneous oscillation of three longitudinal modes. *Optics & Laser Technology*, *44*(7), 2135-2139.

Malos, J. T., Tang, D. Y., & Heckenberg, N. R. (1998). Dependence of transient dynamics in a class-C laser upon variation of inversion with time. *Physical Review A*, *57*(1), 559.

Balkanski, M., & Wallis, R. F. (2000). *Semiconductor physics and applications* (Vol. 8). Oxford University Press..

Dupuis, R. U. S. S. E. L. L. D. (1987). An introduction to the development of the semiconductor laser. *IEEE Journal of Quantum Electronics*, *23*(6), 651-657.Basov *et al.*, 1961; Bernard and Duraffourg, 1961; Hall *et al.*, 1962; Nathan *et al.*, 1962)

Krivtsun, I., Korzhyk, V., Nesterenkov, V., & Kvasnytskyi, V. (2023). Laser welding and cutting. In *Welding of Metallic Materials* (pp. 113-148). Elsevier..

Ahmed, M., & Al-Alhumaidi, M. (2023). Influence of carrier transport on modulation characteristics of quantum-well semiconductor lasers. *Journal of Computational Electronics*, *22*(4), 1140-1150.

Chen, T., Liu, Z., Yang, Q., Meng, J., Wang, T., He, J. J., ... & Li, M. (2023). 4* 10 Gbps WDM communication system based on a tunable V-cavity semiconductor laser. *Optics Express*, *31*(17), 28174-28184.

Kamberaj H. (2023). Viewpoint: The Physics in the New Era of Computing. European Scientific Journal, ESJ, 19 (15), 1

Wang, Y., Huang, Y., Zhou, P., & Li, N. (2023). Dual-Channel Secure Communication Based on Wideband Optical Chaos in Semiconductor Lasers Subject to Intensity Modulation Optical Injection. *Electronics*, *12*(3), 509.

Iga, K., & Li, H. E. (2003). Vertical-cavity surface-emitting laser devices. *Cham, Switzerland: Springer*.

Diode Laser: The Most Versatile and Convenient Coherent Light Source, https://www.findlight.net/blog/diode-laser/, 16 Jan, 2024.

Alferov, Z. I. (1969). AlAs-GaAs heterojunction injection lasers with a low room-temperature threshold. *Fiz, Tekh. Poluprov*, *3*, 1328-1332.

Hayashi, I., Panish, M. B., Foy, P. W., & Sumski, S. (1970). Junction lasers which operate continuously at room temperature. *Applied Physics Letters*, *17*(3), 109-111.

Tournié, E., Monge Bartolome, L., Rio Calvo, M., Loghmari, Z., Díaz-Thomas, D. A., Teissier, R., ... & Rodriguez, J. B. (2022). Mid-infrared III–V semiconductor lasers epitaxially grown on Si substrates. *Light: Science & Applications*, *11*(1), 165.

Jia, X., Wang, Y., Liu, G., Zhou, X., Zhang, J., Dong, F., ... & Zhang, R. (2023). Sensing strategy based on random slot semiconductor laser. *Laser Physics*, *33*(7), 076204.

Lee, H., York, P. K., Menna, R. J., Martinelli, R. U., Garbuzov, D. Z., Narayan, S. Y., & Connolly, J. C. (1995). Room-temperature 2.78 μm AlGaAsSb/InGaAsSb quantum-well lasers. *Applied physics letters*, *66*(15), 1942-1944.

Diroll, B. T. (2020). Colloidal quantum wells for optoelectronic devices. *Journal of Materials Chemistry C*, *8*(31), 10628-10640.

Yoshida, H., Yamashita, Y., Kuwabara, M., & Kan, H. (2008). A 342-nm ultraviolet AlGaN multiple-quantum-well laser diode. *nature photonics*, *2*(9), 551-554.

O'Brien, David. "Sensitivity of Quantum Dot Lasers to External Optical Feedback." PhD diss., University College, Cork, Ireland.

Bimberg, D., Grundmann, M., & Ledentsov, N. N. (1999). *Quantum dot heterostructures*. John Wiley & Sons.

Liu, G. T., Stintz, A., Li, H., Malloy, K. J., & Lester, L. F. (1999). Extremely low room-temperature threshold current density diode lasers using InAs dots in In0. 15Ga0. 85As quantum well. *Electron. Lett*, *35*(14), 1163-1165.

Mao, J., Liu, Z., & Ren, Z. (2016). Size effect in thermoelectric materials. *npj Quantum Materials*, *1*(1), 1-9.

Yacomotti, A. M., Denis, Z., Biella, A., & Ciuti, C. (2023). Quantum Density Matrix Theory for a Laser Without Adiabatic Elimination of the Population Inversion: Transition to Lasing in the Class-B Limit. *Laser & Photonics Reviews*, *17*(1), 2200377.

Pieroux, D., & Mandel, P. (1997). On the rate equation approximation for free-running multimode lasers. *Quantum and Semiclassical Optics: Journal of the European Optical Society Part B*, *9*(3), L17.

Xie, Z., Zeng, W., Li, P., Yan, H., & Han, D. (2023). Thermal modulation of a chaotic fiber laser by using a phase-shifted fiber Bragg grating. *IEEE Photonics Journal*.

Abu Saa Muayad, Simultaneous Two State Operation in Quantum Dot Lasers, Thesis submitted in fulfilment of the requirements for the award of the degree of Doctor in Sciences, Vrije university Brussel,2015.

Coldren, L. A. (1997). Diode lasers and photonic integrated circuits. *Optical Engineering*, *36*(2), 616.

Van Tartwijk, G. H. M., Levine, A. M., & Lenstra, D. (1995). Sisyphus effect in semiconductor lasers with optical feedback. *IEEE Journal of Selected Topics in Quantum Electronics*, *1*(2), 466-472.

Lang, R., & Kobayashi, K. (1980). External optical feedback effects on semiconductor injection laser properties. *IEEE journal of Quantum Electronics*, *16*(3), 347-355.

Hohl, A., & Gavrielides, A. (1999). Bifurcation cascade in a semiconductor laser subject to optical feedback. *Physical Review Letters*, *82*(6), 1148.

Tchakounte, F. M., Tchepemen, N., & Nana, L. (2023). Delayed feedback control on wave dynamics in a nonlinear optical cavity with third-order chromatic dispersion. *Results in Physics*, *52*, 106762.

Meucci, R., Llibre, J., Pugliese, E., & Ginoux, J. M. (2023). Dynamics of two-level laser models with cavity loss modulation and delayed feedback. *JOSA B*, *40*(8), 2114-2121.

Barve, K., Singh, U., Yadav, P., & Bhatia, D. (2023). Carbon-based designer and programmable fluorescent quantum dots for targeted biological and biomedical applications. *Materials Chemistry Frontiers*, *7*(9), 1781-1802.

Zhou, X., Zhai, L., & Liu, J. (2023). Epitaxial quantum dots: a semiconductor launchpad for photonic quantum technologies. *Photonics Insights*, *1*(2), R07-R07.

Seravalli, L. (2023). Metamorphic InAs/InGaAs quantum dots for optoelectronic devices: A review. *Microelectronic Engineering*, 111996.

Zheng, Y., Xia, G., Lin, X., Wang, Q., Wang, H., Jiang, C., ... & Wu, Z. (2023, February). Experimental Investigation on the Mode Characteristics of an Excited-State Quantum Dot Laser under Concave Mirror Optical Feedback. In *Photonics* (Vol. 10, No. 2, p. 166). MDPI.

Li, J., Liu, J., Liu, D., Tian, W., Jin, S., Hu, S., ... & Jin, Y. (2023). Ultrafast random number generation based on random laser. *Journal of Lightwave Technology*.

Alferov, Z. I., & Kazarinov, R. F. (1963). Semiconductor laser with electric pumping. *Inventor's certificate*, *181737*.

Kroemer, H. (1963). A proposed class of hetero-junction injection lasers. *Proceedings of the IEEE*, *51*(12), 1782-1783.

Bimberg, D., & Pohl, U. W. (2011). Quantum dots: promises and accomplishments. *Materials Today*, *14*(9), 388-397.

Asada, M., Miyamoto, Y., & Suematsu, Y. (1986). Gain and the threshold of three-dimensional quantum-box lasers. *IEEE Journal of quantum electronics*, *22*(9), 1915-1921.

Eaglesham, D. J., & Cerullo, M. (1990). Dislocation-free stranski-krastanow growth of Ge on Si (100). *Physical review letters*, *64*(16), 1943.

Koguchi, N., Takahashi, S., & Chikyow, T. (1991). New MBE growth method for InSb quantum well boxes. *Journal of crystal growth*, *111*(1-4), 688-692.

Leonard, D., Krishnamurthy, M., Reaves, C., DenBaars, S. P., & Petroff, P. M. (1993). Direct formation of quantum-sized dots from uniform coherent islands of InGaAs on GaAs surfaces. *Applied Physics Letters*, *63*(23), 3203-3205.

Kirstaedter, N., Ledentsov, N. N., Grundmann, M., Bimberg, D., Ustinov, V. M., Ruvimov, S. S., ... & Heydenreich, J. (1994). Low threshold, large To injection laser emission from (InGa) As quantum dots. *Electronics Letters*, *30*(17), 1416-1417.

Nörenberg, C., Oliver, R. A., Martin, M. G., Allers, L., Castell, M. R., & Briggs, G. A. D. (2002). Stranski-Krastanov Growth of InN Nanostructures on GaN Studied by RHEED, STM and AFM. *physica status solidi (a)*, *194*(2), 536-540.

Auth, D., Liu, S., Norman, J., Bowers, J. E., & Breuer, S. (2019). Passively mode-locked semiconductor quantum dot on silicon laser with 400 Hz RF line width. *Optics Express*, *27*(19), 27256-27266.

Huyet, G., O'Brien, D., Hegarty, S. P., McInerney, J. G., Uskov, A. V., Bimberg, D., ... & SpringThorpe, A. J. (2004). Quantum dot semiconductor lasers with optical feedback. *physica status solidi (a)*, *201*(2), 345-352.

Al Husseini, H. B. (2016). Control of nonlinear dynamics of quantum dot laser with external optical feedback. *Journal of Nanotechnology in Diagnosis and Treatment*, *4*, 5-14.

Jiang, Z. F., Wu, Z. M., Jayaprasath, E., Yang, W. Y., Hu, C. X., & Xia, G. Q. (2019, May). Nonlinear dynamics of exclusive excited-state emission quantum dot lasers under optical injection. In *Photonics* (Vol. 6, No. 2, p. 58). MDPI.

Wang, X. H., Wu, Z. M., Jiang, Z. F., & Xia, G. Q. (2021, July). Nonlinear dynamics of two-state quantum dot lasers under optical feedback. In *Photonics* (Vol. 8, No. 8, p. 300). MDPI.

Tykalewicz, B., Goulding, D., Hegarty, S. P., Huyet, G., Dubinkin, I., Fedorov, N., ... & Kelleher, B. (2016). Optically induced hysteresis in a two-state quantum dot laser. *Optics letters*, *41*(5), 1034-1037.

Yamasaki, K., Kanno, K., Matsumoto, A., Akahane, K., Yamamoto, N., Naruse, M., & Uchida, A. (2021). Fast dynamics of low-frequency fluctuations in a quantum-dot laser with optical feedback. *Optics Express*, *29*(12), 17962-17975.

Newell, T. C., Bossert, D. J., Stintz, A., Fuchs, B., Malloy, K. J., & Lester, L. F. (1999). Gain and linewidth enhancement factor in InAs quantum-dot laser diodes. *IEEE Photonics Technology Letters*, *11*(12), 1527-1529.

Chichibu, S. F., Uedono, A., Onuma, T., Haskell, B. A., Chakraborty, A., Koyama, T., ... & Sota, T. (2006). Origin of defect-insensitive emission probability in In-containing (Al, In, Ga) N alloy semiconductors. *Nature materials*, *5*(10), 810-816.

Erneux, T., & Glorieux, P. (2010). *Laser dynamics*. Cambridge University Press.

Uskov, A. V., Boucher, Y., Le Bihan, J., & McInerney, J. (1998). Theory of a self-assembled quantum-dot semiconductor laser with Auger carrier capture: quantum efficiency and nonlinear gain. *Applied physics letters*, *73*(11), 1499-1501.

Fiore, A., & Markus, A. (2007). Differential gain and gain compression in quantum-dot lasers. *IEEE Journal of Quantum Electronics*, *43*(4), 287-294.

Erneux, T., Viktorov, E. A., & Mandel, P. (2007). Time scales and relaxation dynamics in quantum-dot lasers. *Physical Review A*, *76*(2), 023819.

Malić, E., Ahn, K. J., Bormann, M. J., Hövel, P., Schöll, E., Knorr, A., ... & Bimberg, D. (2006). Theory of relaxation oscillations in semiconductor quantum dot lasers. *Applied physics letters*, *89*(10).

O'Brien, D., Hegarty, S. P., Huyet, G., & Uskov, A. V. (2004). Sensitivity of quantum-dot semiconductor lasers to optical feedback. *Optics letters*, *29*(10), 1072-1074.

Kelleher, B., Goulding, D., Hegarty, S. P., Huyet, G., Viktorov, E. A., & Erneux, T. (2012). Optically injected single-mode quantum dot lasers. *Quantum dot devices*, 1-22. Part of the book series Lecture Notes in Nanoscale Science and Technology, volume 13.

Erneux, T., & FREE UNIV OF BRUSSELS (BELGIUM). (2012). *Stability and Tolerance to Optical Feedback of Quantum Dot Lasers*.

Erneux, T., Viktorov, E. A., Kelleher, B., Goulding, D., Hegarty, S. P., & Huyet, G. (2010). Optically injected quantum-dot lasers. *Optics letters*, *35*(7).

Yamada, M. (2014). *Theory of semiconductor lasers* (Vol. 185).

Oliver, E. C. J. (2004). *Optical Bistability and Soliton Switiching in an Optical Ring Cavity* (Doctoral dissertation, Acadia University)].

Mehmannavaz, M. R., & Sattari, H. (2015). A quintuple quantum dot system for electrical and optical control of multi/bistability in a telecommunication window. *Laser Physics Letters*, *12*(2), 025201].

Ohtsubo, J., & Ohtsubo, J. (2013). Theory of optical feedback in semiconductor lasers. *Semiconductor Lasers: Stability, Instability and Chaos*, 75-101].

Mao, M. H., Wu, T. Y., Wu, D. C., Chang, F. Y., & Lin, H. H. (2004). Relaxation oscillations and damping factors of 1.3 μm in (Ga) As/GaAs quantum-dot lasers. *Optical and quantum electronics*, *36*, 927-933.

الملخص

في هذه الأطروحة، ندرس ليزرات النقاط الكمية التي تستخدم النقاط الكمية كمواد نشيطة. وتعمل ليزرات النقاط الكمية على مبدأ الحبس الضيق لناقلات الشحنة في نقاط الكم ، وتجد مجموعة واسعة من التطبيقات في التصوير الطبي , الاستشعار, معالجة المعلومات الكمية والاتصالات البصرية. ونظرا لدورها الحيوي في معالجة الأمراض والتصوير الضوئي، بالإضافة إلى القدرة العالية في معالجة البيانات، تستخدم نُهج جديدة لتحسين أدائها. ويركز عملنا على المعالجة النظرية للأثار الديناميكية للتغذية الضوئية الراجعة باستخدام نهج معادلة المعدل. وتم اشتقاق صيغة رياضية لكل من تذبذب الاسترخاء ومعدل التثبيط. بالاضافة لذلك، تم استخدام طريقة المحاكاة لمقارنة نتائج هذه الدراسة بنتيجة الليزر الانفرادي. وتبين أن التعقيبات الضوئية تعزز تذبذبات الاسترخاء وتقلل من معدل وعامل التثبيط بزيادة معدل الحقن مما ينتج عنه انخفاض استقرار النظام. وعلاوة على ذلك, تبين وجود منطقة عدم استقرار في النطام دل عليها معدل التثبيط الموجب. بالاضافة لذلك, يوجد منطقة ثنائية الاستقرار والتي تسمح باستخام الليزر كمفتاح ضوبي وفي تخزين المعلومات الضوئية.